Available online at www.sciencedirect.com

SCIENCE DIRECT®

Geochimica et Cosmochimica Acta 70 (2006) 2104–2126

Geochimica

www.elsevier.com/locate/gca

Siderophile geochemistry of ureilites: A record of early stages of planetesimal core formation

Paul H. Warren *, Finn Ulff-Møller, Heinz Huber, Gregory W. Kallemeyn

Institute of Geophysics, UCLA, Los Angeles, CA 90095-1567, USA

Received 23 May 2005; accepted in revised form 2 December 2005

Abstract

New bulk-compositional data, including trace siderophile elements such as Ir, Os, Au, and Ni, are presented for 25 ureilites. Without exception, ureilites have siderophile abundances too high to plausibly have formed as cumulates. Ureilites undoubtedly underwent a variety of "smelting," by which C was oxidized to CO gas while olivine FeO was reduced to Fe-metal. However, pressure-buffered equilibrium smelting is not a plausible model for engendering the wide range (75–96 mol%) of mafic-silicate core *mg* among ureilites. The smelting reaction produces too much CO gas. Even supposing a disequilibrium process with the smelt-gas leaking out of the mantle, none of the ureilites, least of all the ureilite with the most "reduced" (highest) olivine-core *mg* (ALH84136), has the high Fe-metal abundance predicted by the smelted-cores model. In principle, the Fe-metal generated by smelting could have been subsequently lost, but siderophile data show that ureilites never underwent efficient depletion of Fe-metal. Ureilites display strong correlations among siderophile ratios such as Au/Ir, Ni/Ir, Co/Ir, As/Ir, Se/Ir, and Sb/Ir. Ureilite siderophile depletion patterns loosely resemble siderophile fractionations, presumably nebular in origin, among carbonaceous chondrites. However, Zn, for an element of moderate volatility, is anomalously high in ureilites. A tight correlation between Au and Ni extrapolates to the low-Ni/Au side of the compositional range of carbonaceous chondrites. From this mismatch, mild but nonetheless significant depletions of refractory siderophile elements such as Ir and Os, and moderate depletions of strongly siderophile, weakly chalcophile elements such as Ni and Au, we infer that the ureilite siderophile fractionations are largely the result of a non-nebular process, i.e., removal of S-rich metallic melt, possibly with minor entrainment of Fe-metal. Several lines of trace-element evidence indicate that melt porosity during ureilite anatexis was at least moderate. The ureilite pattern of very mild depletions of extremely siderophile elements, but much deeper depletions of moderately siderophile, chalcophile elements, suggests that asteroidal core formation probably occurs in two discrete stages. In general, separation of a considerable proportion (several wt%) of S-rich metallic melt probably occurs long before, and at a far lower temperature than, separation of the remaining S-poor Fe-metal. Apart from the Fe-metal itself, only extremely siderophile elements wait until the second stage to sequester mainly into the core.

1. Introduction

Ureilites are the second most abundant and in many ways the most distinctive (some might say weird) type of achondrite. As reviewed by Mittlefehldt et al. (1998), they are, in essence, extremely depleted peridotites, with typically about 2/3 olivine, 30% pyroxene (mostly pigeonite), and virtually zero observable feldspar. In nearly all cases they also contain carbon (average 3 wt%), usually as intergranular "veins" of semi-amorphous "C-matrix" (often with traces of diamond). In low-shock samples, the intergranular C phase may be euhedral graphite (e.g., Berkley and Jones, 1982). The ureilites were once popularly viewed as igneous cumulates (e.g., Berkley et al., 1980; Goodrich et al., 1987; Walker and Agee, 1988). But the discovery by Clayton and Mayeda, 1988, that ureilites feature enormous oxygen-isotopic diversity, engendered an abrupt shift in ureilite petrogenetic modeling. More recent authors (e.g., Warren and Kallemeyn, 1992; Scott et al., 1993; Walker and Grove, 1993; Singletary and Grove, 2003; Goodrich et al., 2004; Kita et al., 2004) generally assume that most ureilites formed as asteroidal mantle restites.

---

* Corresponding author. Fax: +1 310 206 3051.
E-mail address: pwarren@ucla.edu (P.H. Warren).

0016-7037/$ - see front matter © 2006 Elsevier Inc. All rights reserved.
doi:10.1016/j.gca.2005.12.026

In some important ways, ureilites represent cases of arrested development. Their olivines typically feature reduced rims, i.e., the intergranular C phase has reacted with oxygen from the fayalite component of the olivine to yield high-*mg* (= MgO/[MgO + FeO] in mol%) residual olivine, sprinkled tiny grains of Fe-metal, and high-*mg*, low-Ca pyroxene (e.g., Singletary and Grove, 2003). But this "smelting" process invariably ended before the cores of the olivines could be reduced to nearly the same extent as the rims. Another characteristic feature of ureilites (e.g., Goodrich et al., 1987) is a pattern of moderate (vs. chondrites) siderophile-element depletion that suggests the parent asteroid(s) formed a core, but only to an incomplete extent; i.e., without the efficient separation of metal from silicate that is usually envisaged to result from Earth-style core formation.

In this paper, we utilize new data for ureilite trace siderophile elements, in conjunction with other (e.g., incompatible-element, petrologic) constraints, to gain insight into the early stages of asteroidal core formation. The prerequisites for core formation, in terms of temperature and proportion of melt porosity in an anatectic mantle, are still only vaguely understood. At one extreme, Larimer (1995) has suggested that the entire portion of an asteroid "inside the 1000 °C isotherm…will be swept clean of its metal as well as its sulfide." More recently, Yoshino et al. (2004) have suggested that metallic melt does not percolate out of an anatectic mantle until the total melt porosity exceeds ~35 vol% (where roughly 13 vol% is metallic melt, roughly 20–25 vol% is silicate melt). Ureilite petrology issues, such as the enigmatic depletion of Al (basalt), the possibility that some might be cumulates, and the overall role of smelting, are also constrained by our new results.

2. Data sources, new and old

2.1. Techniques

All samples were studied by instrumental neutron activation analysis (INAA), using the procedure of Kallemeyn (1993). Irradiations were obtained at the UC Irvine reactor facility. Our procedure included a 1-min preliminary "rabbit" activation, followed by rapid, 2-min duration, counting of short-lived nuclides to determine Mg, Al, Ca, Ti, V, and Mn. Other elements, and replicate data for Mn and Ca, were determined after a subsequent 4-h irradiation, through a series of 4–5 separate, increasingly long counts that finally ended about two months after the irradiation. Data analysis was based on the program SPECTRA (Grossman and Baedecker, 1986), which achieves optimal precision through the use of graphic display and interactive analysis of the γ-ray spectra. Integrations of the areas of small γ-ray peaks and multiplets were checked visually, and baseline parameters were adjusted where necessary. Capability of this technique for a given element is a function of nuclear, not chemical (periodic-table), characteristics. For some siderophile elements (e.g., Mo, Rh, and Pt), our variety of INAA is hopelessly insensitive. However, the high, near-chondritic siderophile concentrations typical of ureilites allow INAA to determine some elements (e.g., Re, Os) that it usually cannot, and to determine Ni, Ir, and Au with relatively high precision. In order to fit into our standard plastic INAA vial, some of the largest samples were first crushed in a cylindrical stainless steel device.

Many of the samples, including all five "new" NWA ureilites, were also studied petrographically. Mineral compositions were determined using wavelength-dispersive detectors on an electron probe, either a Cameca Camebax or (more commonly) a JEOL JXA-8200, in all cases at UCLA and running at an accelerating voltage of 15 kV, with count durations of generally 15–20 s.

2.2. Samples

The 25 samples that we chose for analysis were selected, in part, to provide diversity in terms of mafic-silicate-core *mg*, pyroxene type, *py* (= pyroxene/[pyroxene + olivine] in mol%) and texture (Table 1). Most are not paired with any other known meteorite. However, both EET87511 and EET96328 are paired with EET87523, EET87717, EET96262, and EET96322 (Goodrich, 2001). QUE93341 is paired with QUE93336 (Goodrich, 1999). FRO90168 is probably paired with FRO90036 (Smith et al., 2000). NWA1462 and NWA1464 are conceivably paired. Both have Fo_{78} olivine cores. Olivines in NWA1464 have unusually broad reduction rims, accounting, on average, for 2/3 of the original grains; and those in NWA1462 are almost as broad. However, their pigeonites are disparate, $En_{68.0}Wo_{14.3}$ and $En_{76.4}Wo_{8.7}$, respectively. In terms of bulk composition (Table 2), Sc is 1.5× higher in NWA1464; also, highly siderophile elements are significantly lower, and Au/Ni in NWA1464 is only 0.6× the NWA1462 ratio.

Typical sample mass was 400 mg. Three of the largest samples, EET87511, GRA98032, and Y-791538, were first split into two subequal masses for analysis as separate INAA samples. Past work (e.g., Warren and Kallemeyn, 1992), supported by the new results (Table 2; the two EET87511 splits should also be compared with the EET96328 results), indicates that 300–400 mg is sufficient to give a fairly representative analysis for most ureilites.

For most of our samples, no trace-element data was available from previous literature. Wang and Lipschutz (1995) previously analyzed LEW88006 and Y-791538. For both samples, their data for most of the elements in our common repertoire (Co, Zn, Ga, Se, and Sb, but not Au) are systematically ~0.9× low compared to ours. In the case of Sb in Y-791538, our two data are higher than their result by large factors (3–6). Apparently, our sample was compromised by Sb contamination.

Table 1 also indicates weathering classifications. The main criterion for these evaluations is rusting of metallic phases (Wlotzka, 1993). However, judging from various

Table 1
Mineralogical and petrological characteristics of analyzed ureilites

	Total known wt. (g)	Olivine cores				mol% *py*	Unusual mineralogy?	Unusual texture?	Weathering class	References
		mg	CaO	Cr_2O_3	*N*					
Antarctic										
Asuka 881931,63	153.6	76	—	—	—	15			W1^{a}	Yanai and Kojima (1995)
EET87511,20a		(see EET87511,20b)								
EET87511,20b	65.1	85.1	0.31	0.63	32^{a}	54	Opx + augite	Bimodal	B	AMN 11(2)
EET96328,7	7.1	(see EET87511)								
EET90019,5	21.5	89.3	0.34	0.62	12^{a}	40			B/Ce	AMN 15(1)
EET96001,5	5.8	81.5	0.37	0.59	149^{a}	10	Trace plag		B	AMN 21(1)
FRO90054,5	17.51	87	—	—	—	66	Opx + augite		W0	MetBul 73
FRO90168,3	14.26	79	—	—	—	55	Opx + augite	Mosaicized	A/B^{b}	MetBul 77
GRA95205,28	1460	79.0	0.27	0.60	35^{a}	5	Opx; low *py*		B	AMN 20(1)
GRA98032,28a GRA98032,28b	1700	76.6	0.36	0.69	11^{a}	10^{a}	Augite	Mosaicized	C	AMN 23(1)
GRO95575,13	138	79	0.39	0.83	—	9			A/B	Singletary and Grove (2003)
LEW88006,16	27	82	—	—	—	—			B	AMN 13(2)
LEW88774,7	3.1	74.9	0.23	0.37	7^{a}	87	Opx + augite		B/C	AMN 16(1)
MET01083,8	12.6	91.9	0.30	0.48	5^{a}	—			B	AMN 25(2)
MET01085,13	30.6	No olivine				100	No olivine		B	AMN 25(2)
QUE93341,14	7.5	78	0.30	0.56	—	40			B	Singletary and Grove (2003)
Y791538,89a Y791538,89b	419	91	—	—	—	45	Opx + pig		W1^{a}	Yanai and Kojima (1995)
Warm-desert										
El Gouanem	2100	76.5	—	—	—	18			W2^{a}	MetBul 85
HAH 126	1998	79.7	0.36	0.69	20^{a}	32			W3	MetBul 80
Hughes 009	108	87	0.29	0.55	—	70	Opx + augite, etc.		W3^{a}	Goodrich et al. (2001)
NWA766	309	76.3	0.26	0.42	35^{a}	25^{a}	Cr-silicates, etc.		W2^{a}	Warren (2004)
NWA1006	24.5	89.6	0.33	0.64	47^{a}	40^{a}	Opx + pig^{a}		W2^{a}	This work
NWA1462	203	78.1	0.30	0.50	10^{a}	30^{a}			W1^{a}	This work
NWA1464	1800	77.7	0.31	0.45	19^{a}	30^{a}			W3^{a}	MetBul 87; this work
NWA2225	40	82.3	0.36	0.71	18^{a}	25^{a}			W3^{a}	This work
Reid 016	110	Diverse				Diverse		Polymict	W2^{a}	MetBul 82

Abbreviations: mg, MgO/(MgO + FeO) in wt%; *N*, number of olivine-core analyses averaged (averages exclude a typically larger number of high-*mg* analyses from closer to reduced rim); py, pyroxene/(pyroxene + olvine) in mol%; opx, orthopyroxene; plag, plagioclase; AMN, Antarctic meteorite Newsletter; MetBul, meteoritical bulletin; and HAH, Hammadah al Hamra.

[a] This work (weathering classifications after Wlotzka, 1993).

[b] FRO90036 is weathering class B/C.

correlations among siderophile elements, to be discussed at length below, the effects of even relatively severe ("C") Antarctic weathering are surprisingly benign for these elements. Besides the various diagrams that we show later in this paper, we constructed plots (not shown) of Ir, Ni, and Au/Ir plotted against weathering scale. No significant effect of weathering was manifest for data sets limited to falls, fresh finds and Antarctic samples. Apparently, even extensive Antarctic oxidation does not necessarily imply major transport of siderophile elements. The warm-desert ureilites, however, are another story. With them, it seems that even moderate oxidation is typically accompanied by significant transport of at least some of the siderophile elements. In general, however, it seems that the worst effects involve addition more than removal, and the most severely affected siderophile elements are ones that are partially chalcophile and only weakly to moderately siderophile, such as, among our analytical repertoire, As, Sb, and especially Br.

For the remainder of this paper, we shall not confine our interpretation to the new analyses (Table 2) alone. Where reference is made to the geochemical characteristics of individual ureilites, or to ureilites as a sample population, unless otherwise noted the reference is to the complete literature data set (averaged, for individual samples). For siderophile and chalcophile elements, the literature averages are summarized in Table 3. Note that Te, Tl, and Bi concentrations also tend to be far higher in warm-desert weathered ureilites than in unweathered samples.

Among the individual ureilites studied, MET01085 stands out because it is devoid of olivine and so arguably might not be a "real" ureilite. However, a 31-g ($\sim$10 cm^3) sample might be far from ideally representative of the larger-scale mineralogy of the parent material. McCoy et al. (2002) noted the presence of carbonado, a typical ureilite component. The minor element composition of the pyroxene (Table 4) almost precisely matches pyroxenes of similar EnFsWo proportions from known ureilites. TiO_2 is very

Table 2
Concentrations of 37 elements in bulk-rock samples of ureilites

	Mass (mg)	Na (mg/g)	Mg (wt%)	Al (wt%)	K (mg/g)	Ca (wt%)	Sc (μg/g)	Ti (mg/g)	V (μg/g)	Cr (mg/g)	Mn (mg/g)	Fe (wt%)	Co (μg/g)	Ni (μg/g)	Zn (μg/g)	Ga (μg/g)	As (μg/g)	Se (μg/g)	Br (μg/g)	Ru (ng/g)	Sb (ng/g)	Ba (μg/g)	La (ng/g)	Ce (ng/g)	Nd (ng/g)	Sm (ng/g)	Eu (ng/g)	Tb (ng/g)	Ho (ng/g)	Yb (ng/g)	Lu (ng/g)	Hf (ng/g)	Re (ng/g)	Os (ng/g)	Ir (ng/g)	Au (ng/g)	Th (μg/g)	U (μg/g)
Normal uncertainty[a]		3%	7%	5%	10%	5%	3%	10%	5%	3%	5%	4%	4%	4%	4%	5%	6%	8%	7%	9%	9%	12%	5%	10%	10%	5%	7%	11%	11%	11%	12%	11%	9%	10%	4%	5%	10%	12%
Asuka 881931,63	517	0.73	19.2	0.41	0.35	1.27	10.3	<1.0	111	4.41	2.8	11.9	74	820	260	2.39	0.19	2.1	1.41	<270	9	<30	21	<200	<500	19	9	<20	26	78	14.1	<30	<30	108	105	14.9	<0.05	<0.012
Notable uncertainty[a]																6					29		21				33		13					12				
EET87511,20a	301	0.28	19.8	0.31	<0.010	0.77	7.9	—	99	4.80	3.1	9.9	27	276	230	1.42	<0.18	0.24	0.34	<160	90	<20	<60	<400	<800	9	<50	<30	<270	37	9	<700	—	—	93	5.3	<0.05	<0.11
Notable uncertainty[a]																		30	38							27				27	33					7		
EET87511,20b	304	0.26	21.1	0.27	<0.018	0.80	8.2	0.4	99	5.0	3.3	9.3	21	196	260	1.15	0.05	0.19	0.42	<212	115	<30	<30	<800	<400	5.9	<5	<40	<28	38	6.5	<50	—	<150	74	4.2	<0.05	<0.025
Notable uncertainty[a]								30									22	30								10					21							
EET96328,7	360	0.24	24.2	0.40	<0.06	0.65	7.0	<0.6	113	4.54	3.2	8.3	21	231	250	1.36	0.04	0.36	1.40	<400	<10	<20	<20	<400	<400	4.1	5.3	<10	<150	28	8.5	<40	<30	119	109	6.4	<0.05	<0.012
Notable uncertainty[a]																10	22	14								13	26			14	13							
EET90019,5	540	0.24	21.3	0.24	<0.015	0.75	7.9	<0.5	93	4.09	3.1	9.4	139	1690	330	2.25	0.43	0.70	0.41	340	14	<30	20	<600	<800	20	<30	<60	19	82	11.3	<100	<50	290	260	42	<0.06	<0.016
Notable uncertainty[a]																	15	15	8		20		24						33					12				
EET96001,5	316	0.23	18.9	0.29	<0.014	0.77	6.6	0.3	94	3.23	2.6	11.7	146	2090	200	2.92	0.53	4.0	0.39	500	55	<13	<20	<500	<800	14.9	<4	<200	<50	56	11.6	<80	—	370	340	55	<0.1	<0.03
Notable uncertainty[a]								38			6																			13	14			15				
El Gouanem	562	0.189	17.0	0.121	0.033	0.78	6.3	<0.6	76	4.03	2.8	12.9	91	830	270	1.23	1.05	0.36	0.36	280	24	51	280	620	<400	70	21	<20	17	44	7.0	<30	—	200	169	10.5	<0.04	0.025
Notable uncertainty[a]																		13											23	14	15			20				26
FRO90054,5	414	0.76	17.5	0.66	<0.13	4.7	24.3	0.96	151	5.4	3.2	11.0	80	1260	92	5.40	0.13	2.6	1.37	<700	16	<20	74	<500	<500	144	40	37	79	210	39	<140	<40	123	117	19.1	<0.1	0.25
Notable uncertainty[a]								23									20				30		6				9	35	20					15				
FRO90168,3	378	0.69	20.9	0.33	<0.12	0.86	7.7	<0.5	86	3.83	2.8	13.9	143	1670	200	2.44	0.25	1.8	2.0	400	12	<30	16	<400	<1000	20.8	13	<30	22	82	11.8	<70	<160	400	330	36	<0.1	0.025
Notable uncertainty[a]																					29		35				20											
GRA95205,28	447	0.28	21.3	0.26	<0.07	0.51	6.3	<0.6	101	4.36	2.8	12.2	117	1350	181	1.83	0.23	1.00	2.1	460	15	<40	<50	<300	<1200	5.6	9.2	<20	<50	24	7.4	<80	<180	450	390	26	<0.1	<0.04
Notable uncertainty[a]																7	12				31					25	15			31	30							
GRA98032,28a	483	0.145	18.7	0.188	<0.03	0.65	7.0	<0.7	86	4.61	2.78	15.9	93	760	250	1.25	0.15	0.24	0.28	380	16	<20	<100	<200	<600	<5	<6	<100	<50	<50	4.8	<100	21	310	234	19.9	<0.1	<0.04
Notable uncertainty[a]																	16	12	9	12	30										29		14					
GRA98032,28b	496	0.154	18.0	0.197	<0.03	0.77	7.0	<0.6	89	4.42	2.73	15.2	105	910	220	1.63	0.20	0.19	0.28	340	66	<20	<100	<400	<500	<3	<7	<100	<40	26	9.5	<60	27	340	272	24	<0.1	<0.04
Notable uncertainty[a]																		13		13										25	16							
GRO95575,13	449	0.163	20	0.217	<0.07	0.98	8.1	<0.4	111	4.92	2.9	11.6	55	490	174	1.91	0.085	0.64	2.2	290	<20	<30	<10	<300	<500	<10	4.9	<20	<60	28	8.6	<60	<120	260	221	10.8	<0.08	<0.013
Notable uncertainty[a]																											14			24	17							
Hammadah 126	312	0.201	20	0.070	0.07	0.97	6.5	—	109	4.85	3.1	15.2	89	860	185	1.11	0.97	0.38	0.59	<1000	17	250	151	<500	<800	23	<12	<90	<40	30	<13	<40	<100	200	199	11.5	0.14	0.29
Notable uncertainty[a]					19											15		30			35									28				20			23	
Hughes 009	386	0.69	14.3	0.56	0.24	2.98	19.9	0.69	122	5.7	3.2	14.8	87	1910	78	5.30	0.36	4.9	2.8	<500	50	35	790	2100	1110	240	73	41	<150	190	35	70	<70	120	101	21.2	0.14	<0.05
Notable uncertainty[a]								23									22				19	14			14			17				20		16			25	
LEW88006,16	343	0.175	19.0	0.33	<0.06	1.30	11.5	<1.1	128	5.4	3.1	12.0	43	540	360	3.04	<0.3	0.66	1.8	300	<60	<30	<200	<200	<500	<20	<15	<20	<130	59	12.7	<30	<70	169	131	17.7	<0.05	<0.1
Notable uncertainty[a]																		9												21	14							
LEW88774,7	283	2.70	13.9	1.29	0.12	3.30	21.5	0.80	420	43.0	3.7	14.7	146	1690	300	28.7	0.43	1.48	9.5	570	23	—	168	<500	<600	146	40	—	—	380	62	80	—	480	480	34	—	—
Notable uncertainty[a]																	11			14	25											21		13				
MET01083,8	341	0.36	21.1	0.34	<0.03	2.98	10.27	<0.9	142	3.74	1.90	7.0	80	910	71	1.80	0.14	<0.9	0.27	202	17	<20	<100	<400	<500	97	9.8	<50	12	36	5	<40	8.7	120	99	19.0	<0.1	<0.03
Notable uncertainty[a]																				23	16						18		28	17	38		21	12				
MET01085,13	402	0.50	16.0	0.61	<0.05	1.41	15.0	0.8	99	4.84	3.2	6.2	25	380	104	2.90	0.10	0.67	0.15	<400	23	<30	15	<300	<1000	31	15	21	40	157	30	<100	13.1	220	192	11.7	<0.1	<0.03
Notable uncertainty[a]								29									10				11		23				8	20					18	11				
NWA766	513	1.27	17.5	0.44	0.18	1.16	8.7	<2	86	4.49	2.8	14.7	100	1040	340	2.53	0.77	0.68	0.48	<840	17	130	930	1710	500	196	62	<40	38	130	21	58	—	190	187	7.6	0.05	0.057
Notable uncertainty[a]																		9			29				32				24			25		25			29	
NWA1006	472	0.158	18.3	0.29	0.11	13.2	9.4	<0.5	101	4.40	2.7	6.4	68	720	330	1.29	0.49	<0.7	0.16	200	60	48	180	<350	<700	30	6.2	<20	20	79	11	<50	—	107	124	16.1	<0.05	0.030
Notable uncertainty[a]																			12		10						29		33		19			25				25
NWA1462	454	0.51	18.6	0.34	<0.04	1.44	9.4	<0.7	81	3.66	3.0	13.3	97	900	159	2.05	0.32	0.35	0.64	399	15	<20	<100	<200	<500	9.3	9	<100	<100	60	11.4	<100	<20	380	360	31	<0.1	<0.04
Notable uncertainty[a]																	9	10		21	35					9	30				13							
NWA1464	365	0.80	19.0	0.56	0.17	2.07	14.3	<1.1	109	4.89	3.6	14.5	92	860	210	2.80	1.20	0.52	0.71	<1700	73	210	3000	6700	3000	690	154	84	121	260	45	<150	20	230	287	17.5	0.24	0.23
Notable uncertainty[a]																20		12															30	*15*			20	
NWA2225	456	0.187	18.4	0.228	0.17	1.49	70	<0.8	95	4.56	3.0	12.8	118	1140	280	1.43	1.60	0.34	0.47	779	250	71	740	1890	<800	146	33	<20	<60	88	21	87	<20	190	231	9.8	0.12	0.057
Notable uncertainty[a]																10				6											12							25
QUE93341,14	364	0.44	20.7	0.32	0.042	0.99	9.7	<0.8	101	4.29	2.9	13.6	139	1550	175	3.16	0.33	1.19	2.2	540	<100	<50	<200	<200	<400	10	9.6	<40	<60	54	13.9	<70	<110	460	420	35	<0.1	<0.3
Notable uncertainty[a]					15												12									37	18											
Reid 016	426	0.49	16.5	0.31	0.094	1.15	8.2	<2	97	4.46	2.7	15.6	220	2650	210	2.80	0.67	1.10	1.15	765	19	47	1340	2800	1100	310	86	45	45	131	18	<60	<50	800	640	45	0.08	0.046
Notable uncertainty[a]																		11			22				18			13						10			13	22
Y791538,89a	261	0.27	19.0	0.27	0.022	1.28	11.4	—	100	4.44	3.1	7.7	105	1280	240	2.54	0.32	0.60	0.62	—	80	<30	<70	<290	<1100	16	<12	<200	<400	104	18	<60	—	250	230	32	<0.07	<0.3
Notable uncertainty[a]					31												23	15	21		18					22				13	16							
Y791538,89b	272	0.28	20.6	0.24	0.009	1.48	11.8	<0.5	101	4.75	3.4	7.7	103	1220	290	2.83	0.33	0.55	0.76	240	150	<13	<60	<510	<800	15.3	<10	<50	<300	112	18	<60	—	300	233	34	<0.05	<0.06
Notable uncertainty[a]			15		19													11								6								25				

[a] Uncertainties are shown where they are larger than normal 70% confidence levels (i.e., ''normal'' for moderate-high concentrations).

Table 3

Summary of averaged literature[a] data for siderophile and "chalcosiderophile" elements in ureilites

Meteorite	Olivine Fo	C (μg/g)	Co (μg/g)	Ni (μg/g)	Zn (μg/g)	Ge (μg/g)	As (μg/g)	Se (μg/g)	Br (μg/g)	Mo (ng/g)	Ru (ng/g)	Pd (ng/g)	Ag (ng/g)	Cd (ng/g)	In (ng/g)	Sb (ng/g)	Te (ng/g)	W (ng/g)	Re (ng/g)	Os (ng/g)	Ir (ng/g)	Pt (ng/g)	Au (ng/g)	Tl (ng/g)	Pb (ng/g)	Bi (ng/g)	Siderophile data sources
Acfer 277	79	24	91	749	—	—	—	—	—	—	—	—	—	—	—	—	—	—	32	343	244		17	—	—	—	BH93
ALH77257	85	33	97	910	267	—	0.20	0.26	—	—	230	—	1.9	4.9	0.36	13	22	40	10	150	180	—	20	—	—	—	WK92, SB91, S92, WL95, K
ALH78019/262	77.5	—	134	800	331	—	0.20	1.64	—	—	610	—	—	15	6.4	24	195	106	61	880	438	—	30	12.2	—	0.52	WK92, S92,WL95, K
ALH81101	79	—	62	750	148	—	0.10	1.19	—	—	300	—	8.5	3.7	1.71	13	88	7.7	4.7	45	38	—	12	0.63	—	0.72	WK92, SB91, WL95
ALH82106/130/4136	95.5	25	106	1388	223	—	0.28	1.05	—	—	250	—	7.6	3.3	0.99	15	37	25	10	162	157	—	36	0.17	—	1.12	WK92, SB91, WL95, K
Dingo Pup Donga	84	27	181	2800	230	—	—	2.98	—	—	—	—	—	—	—	—	—	—	—	—	—	—	—	—	—	—	MC68, K
Dyalpur	84	24	106	1270	276	9.6	—	0.69	0.20	—	—	—	57	32	1.10	28	52	—	16	—	221	—	31	2.11	—	1.78	B75, H76, W76, S92
EET83309	—	24	101	1745	254	11.3	0.39	1.75	0.17	—	398	—	12	22	0.78	23	83	—	11	280	260	—	33	1.94	—	2.40	Table 2, WL95
EET87511 and pairs	85	—	42	234	215	—	0.043	0.26	0.72	460	300	—	—	5.8	1.29	<20	—	25	<30	119	83	—	5.3	—	300	—	Table 2, S92, WL95
EET87720	—	18	128	2165	148	—	0.27	2.68	0.26	—	300	—	34	5.8	1.29	36	308	—	—	<130	88	—	27	0.29	—	2.10	WK92, WL95
FRO90036/168	80	—	140	1798	202	—	0.25	1.77	2.0	—	400	—	—	—	—	12	—	—	28	362	276	—	38	—	—	—	Table 2, BH93
FRO90054	87	2.4	73	1217	92	—	0.13	2.60	1.4	—	<700	—	—	—	—	16	—	—	18	147	104	—	19	—	—	—	Table 2, BH93
Goalpara	79	7	85	874	60	3.8	—	1.19	0.023	—	—	—	10	9.0	0.91	8.4	53	—	6.8	—	71	—	16	1.27	—	1.45	J70, S72, B75, H76, W76, K
Haverö	79	19	116	1094	163	8.6	—	0.79	0.046	—	—	60	27	58	1.09	8.6	54	180	25	—	222	410	21	3.96	—	1.50	G72, W72, B75, H76, W76, H78, S91, K
Kenna	79	24	176	1548	211	22.9	—	0.49	0.15	—	—	—	—	31	1.75	9.8	—	110	60	704	627	—	39	—	—	—	B76, W76, J87, SB91, K
LEW85328	80	37	63	—	163	—	—	1.68	—	—	—	—	18	24	0.51	16	174	—	—	—	60	—	20	1.24	—	1.64	S92, WL95
LEW85440 and pairs	92	—	56	—	191	—	—	1.15	—	800	—	—	11	9.8	1.28	10.8	100	89	—	—	155	—	29	0.79	—	1.46	S92, WL95
LEW88006	82	—	38	544	334	—	—	0.63	1.85	—	300	—	6.8	20	0.51	5.9	60	—	<70	169	131	—	18	2.40	—	2.45	Table 2, WL95
MET78008	77	15	116	1215	260	—	0.25	0.51	—	1300	355	—	4.9	34	0.81	14	33	—	—	405	340	—	22	1.47	—	7.20	WK92, S92, WL95
Nilpena	—	27	146	2000	—	—	—	—	—	—	—	—	—	—	—	—	—	—	—	—	—	—	—	—	—	—	JF82, K
North Haig	—	54	112	1550	230	—	—	1.65	—	—	—	—	—	120	<2	—	—	—	—	—	—	—	—	—	—	—	MC68, B75, J90
Novo Urei	79	26	134	1329	239	10.8	—	0.70	0.01	—	—	—	6.1	19	1.75	6.8	60	93	40	530	427	—	44	0.35	—	6.70	B75, SB91, B76, H76, W76, K
PCA82506	78	45	95	828	222	—	0.19	0.41	—	150	300	—	3.5	14	0.72	10.4	17	40	14	212	177	—	19	0.10	—	0.72	J90, SB91, S92, WK92, WL95, K
RKP80239	83	62	77	840	220	—	0.18	0.44	—	—	280	—	—	—	—	18	—	—	—	221	167	—	17	—	—	—	WK92
Roosevelt County 027	79	—	175	1830	335	—	—	—	—	—	—	—	—	—	—	—	—	—	—	—	580	—	41	—	—	—	G87
Y74123	79	30	170	1600	—	—	—	—	—	—	—	—	—	—	—	—	—	—	—	—	—	—	—	—	—	—	H78
Y790981	78	26	110	2100	222	—	—	2.70	—	2000	—	—	22	25	1.08	23	251	40	—	—	140	—	43	0.66	—	2.57	WL95, K
Y791538	91	31	96	1250	253	—	0.32	0.52	0.69	—	300	—	38	6.3	0.45	<100	83	—	—	300	231	—	32	0.10	—	0.94	Table 2, WL95
Y8448	78	—	61	—	208	—	—	1.23	—	—	—	—	18	23	0.75	9.2	126	—	—	—	—	—	14	0.83	—	0.84	WL95
Avg. little-weathered[b]	—	26	97	1126	193	11.1	0.20	1.07	0.087	930[c]	342	60	17	19	1.10	16	55	65	18.8	279	222	410	25	0.77	530[c]	1.32	
Avg., all ureilites[b]	—	29	104	1267	218	11.2	0.40	1.23	0.81	930[c]	367	60	17	23	1.28	28	100	69	22.4	301	243	410	25	1.8	530[c]	2.1	

Abbreviations: B75, Binz et al. (1975); B76, Boynton et al. (1976); BH93, Boynton and Hill (1993); G72, Gillum et al. (1972); G87, Goodrich et al. (1987); H76, Higuchi et al. (1976); H78, Hintenberger et al. (1978); J70, Jerome (1970); J87, Janssens et al. (1987); J90, Jarosewich (1990); JF82, Jaques and Fitzgerald (1982); K.U. Krahenbuhl (unpublished); MC68, McCall and Cleverly (1968); S72, Schmitt et al. (1972); S92, Spitz (1992); SB91, Spitz and Boynton (1991); W72, Wiik (1972); W76, Wasson et al. (1976); WK92, Warren and Kallemeyn (1992); and WL95, Wang and Lipschutz (1995).

[a] Does not include samples from Table 2 (except where averaged with older literature data); also does not include a few instances where only Ni and/or Co have been determined by wet-chemical analyses.

[b] These averages include many additional samples (with data exclusively from this work) shown in Table 2. For working definition of "little-weathered," see text.

[c] The averages for Mo and Pb are based on a diagram in Spitz (1992) wherein individual samples cannot (in general) be identified, albeit the average is fairly clear.

Table 4
Concentrations of 10 elements in low-Ca pyroxenes of MET01085 and similar ureilites, determined by *e*-probe

Sample	Na_2O	MgO	Al_2O_3	SiO_2	K_2O	CaO	TiO_2	Cr_2O_3	MnO	FeO	Total	En	Fs	Wo	*mg*
MET01085 average[a]	0.05	31.73	1.07	55.74	0.01	2.38	0.129	0.94	0.52	7.20	99.76	84.66	10.77	4.57	88.71
Standard deviation	0.01	0.20	0.04	0.29	0.01	0.04	0.025	0.04	0.03	0.12	—	—	—	—	0.18
EET96293 (Singletary)[a]	—	31.0	1.03	57.5	—	2.32	0.10	0.81	0.56	7.65	101.0	83.88	11.61	4.51	87.8
EET96314 (Singletary)[a]	—	31.2	1.15	56.6	—	2.48	0.11	1.00	0.48	8.0	101.0	83.27	11.98	4.76	87.4
NWA1006 pigeonite[a]	0.03	31.11	0.57	56.08	0.01	4.15	0.115	0.99	0.47	6.21	99.74	82.79	9.27	7.94	89.9
NWA1006 opx[a]	0.02	32.74	0.62	56.17	—	2.48	0.14	0.95	0.45	5.99	99.55	86.43	8.87	4.70	90.7

[a] Data sources: MET01085, average, 97 analyses; EET96293 and 96314, Singletary and Grove (2003); NWA1006, average of 17 very similar analyses of pigeonite, 3 very similar analyses of orthopyroxene.

marginally higher than in any of the comparison pyroxenes, but among Wo ~ 5 ureilitic pyroxenes, that of Y-74130 (which, however, is distinctly ferroan, $mg = 79$: Takeda, 1987) shows a precise match (0.13 wt% TiO_2).

Mineralogically, LEW88774 and NWA766 are extraordinary. They are among the most FeO-rich of ureilites, and both feature chromite, a rare phase among ureilites, plus highly unusual Cr-silicates. The Cr-silicates, which tend to occur in tiny necklace-like chains around chromite (typically separated from the chromite by Si-rich glass), were originally (Goodrich and Harlow, 2001; Sikirdji and Warren, 2001) interpreted as shock-generated Cr-garnets. However, at least in the case of NWA766, more careful study indicates that the Cr-silicate phase is unlikely to be garnet; the Cr is preponderantly Cr^{2+}, not Cr^{3+}, and the stoichiometry is closer to olivine than to garnet (Warren, 2004).

3. Scarcity of aluminum (basalt)

The consistently low Al contents of ureilites led Warren and Kallemeyn (1992) and Scott et al. (1993) to suggest that the basaltic components of the parent asteroid(s) were efficiently lost by a process of explosive volcanism. Wilson and Keil (1991) earlier proposed a similar model for aubrites. These authors noted that eruption of basalt at the surface of a low-gravity, atmosphereless body leads to explosive expansion of any gas bubbles; depending upon assumed volatile content of the erupting magma (and ureilites obviously formed in an environment with abundant potential CO), the explosive force might easily suffice to propel nearly all of the silicate melt clear away from the feeble gravitational bond to the asteroid.

A few ureilites have recently been found that reportedly contain traces of Na-rich plagioclase (Table 1; Bland, 1993; Warren et al., 2006). Our new results (Table 2) basically uphold the pattern of low Al in ureilites, but samples such as LEW88774 and the plagioclase-bearing FRO90054 lead to an average, using only the new data, of 0.38 wt% for 24 non-polymict ureilites. This average is 2.5× the average derived, including literature data, from 16 non-polymict ureilites by Warren and Kallemeyn (1992). The disparity may be a fluke related to the small number of samples (and the most Al-rich samples tend to be small in total mass; LEW88774 is just 3.1 g; Table 1). As discussed by Warren and Kallemeyn (1992), as impact-gardened mixtures, the polymict ureilites might be expected to be richly endowed with whatever basaltic component once formed the crust on the parent asteroid. However, the one "new" polymict ureilite (Reid 016), like its few predecessors (review: Warren and Kallemeyn, 1992), has a bulk Al that closely resembles the non-polymict ureilite average. The total data set for 45 ureilites of all types (Table 2 combined with literature data) now averages 0.30 wt%, still remarkably low in comparison to any plausible chondritic parent material, or in comparison to the average for aubrites (0.48 wt%; Warren and Kallemeyn, 1992). Normalized to CI, the updated ureilite average has Al/Sc depleted to 0.19, and Al/V and Al/Cr depleted to 0.17; if other carbonaceous types (Wasson and Kallemeyn, 1988) are used for the comparisons, these depletion factors only become more pronounced. On balance, the scarcity of Al among all types of ureilites still appears to require gross basalt depletion of the parent asteroid(s), most likely through explosive volcanism.

4. Cumulus processing?

Today, most authors (e.g., Goodrich et al., 2004; Kita et al., 2004) assume that most ureilites formed as asteroidal mantle restites. However, before Clayton and Mayeda (1988) revealed that ureilites as a whole preserve extreme heterogeneity in terms of oxygen isotopes (inconsistent with the homogenization expected after extensive melting), ureilites were commonly assumed to be igneous cumulates (e.g., Berkley et al., 1980; Goodrich et al., 1987; Walker and Agee, 1988). More recently, Goodrich and Keller (2000) have suggested that one unusual ureilite, LEW88774, is a cumulate. Goodrich et al. (2004) suggested that two high-*mg* ureilites formed as "paracumulates," a term coined by Warren and Kallemeyn (1989) to denote "mushy, cumulate-like partial melt residues" that hypothetically might develop within an asteroidal mantle where segregation of melt out of the restite would be hampered by the feebleness of buoyancy forces in the weak local gravity. Also, for the relative few augite-bearing ureilites, and for numerous augite-bearing clasts within polymict ureilites, Ikeda and Prinz (2001) suggested origin as crustal cumulates, and Goodrich et al. (2004) likewise suggested origin as either paracumulates or (conventional) cumulates (with no clear preference between these two alternatives).

Siderophile data militate against formation of any of these rocks as conventional cumulates. In terrestrial literature, a cumulate is a rock formed as an accumulation (Wager and Brown, 1967) or in some models a localized growth-layer (e.g., Hunter, 1996) of liquidus (“cumulus” or “primary precipitate”) crystals close to the margin of a magma that is, at least initially, preponderantly melt. After initial accumulation, the cumulus crystals typically displace most of the interstitial “trapped melt” by compaction and/or continued chemical equilibration with the main reservoir of melt (“adcumulus growth”). Even models that call for cumulates to develop as crystal-rich mushes (Shirley, 1986; Hunter, 1996) envisage the mush as only a narrow compaction zone along the margin of a magma chamber that is melt-dominated. A conventional cumulate model not only starts with production of an extensively molten parent material, it ends by a solid/melt differentiation that is typically highly heterogeneous at all scales—reflecting the vagaries of crystal settling and/or nucleation; and also, at large scales, progressive differentiation of the main mass of melt. A “cumulate sequence” is almost by definition grossly heterogeneous, a “layered intrusion.”

The near-chondritic siderophile abundance levels in ureilites, which distinguish them from virtually all other ultramafic igneous rocks (e.g., Warren et al., 1999), are difficult to reconcile with any model remotely similar to conventional cumulate petrogenesis. During initial melting of an asteroidal interior at low fO_2, highly siderophile elements such as Ir must be concentrated almost quantitatively into S-rich metallic melt and FeNi metal. For FeNi, the low-pressure $D_{\text{Ir-metal/silicate}}$ is estimated to be of order 10^{12} (Borisov and Palme, 1995; cf. Jones et al., 1997). The affinity of Ir for S-rich metallic liquid is more moderate by a factor of up to 2000 (depending upon the S content; Chabot and Jones, 2003), but even so, and even assuming the metallic phase is merely a few tens of μg/g of S-rich melt, all but ~1% of the total Ir should partition into that phase, as opposed to the silicate melt.

Iridium concentrations in ureilites (Tables 2 and 3; Fig. 1) are generally depleted by no more than a factor of 5 vs. CI chondrites. The most extreme depletions, to 0.08–0.16 × CI, occur in three mineralogically nondescript olivine–pigeonite ureilites: ALHA81101, LEW85328 and Goalpara. Texturally, ALHA81101 and Goalpara are shock-metamorphosed, “mosaicized” ureilites, but LEW85328 is “typical” (Mittlefehldt et al., 1998). Five augite-bearing high-*mg* ureilites do show a very marginal tendency toward lower Ir than similarly high-*mg* ureilites without augite (Fig. 1), but the difference is at most a factor of two. The two low-*mg* augite-bearing ureilites, META78008 and LEW88774, have above-average Ir, 0.74–1.04 × CI. The average of all augite-bearing ureilites is only mildly depleted in Ir, to ~0.44 × CI.

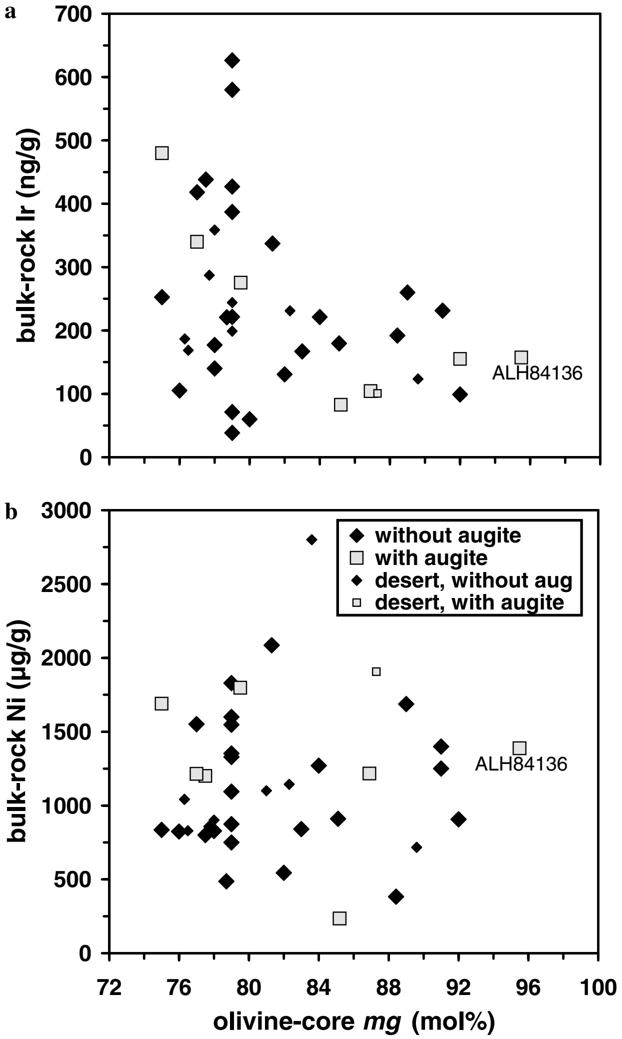

Fig. 1. Olivine-core *mg* vs. bulk-rock data for (a) the extremely siderophile element Ir and (b) the highly siderophile element Ni (*mg* data mainly from review by Goodrich, 1999; Ir data from Table 2 and literature data summarized in Table 3). Darker symbols distinguish little-weathered ureilites from moderately to severely weathered warm-desert ureilites (however, for such highly siderophile elements the two populations do not, with available data, manifest any significant difference). As discussed in text, limited extents of Ni and especially Ir depletions (cf. the CI chondritic Ir concentration, 460 ng/g; Wasson and Kallemeyn, 1988) weigh against cumulate origin, or efficient deplection of Fe-metal during anatexis.

Survival of such near-chondritic Ir concentrations through all the processing required by the cumulate model would be improbable. From phase equilibria of the Fe–FeS system (Usselman, 1975), the S content of the metallic melt might plausibly have ranged from 31 wt% at the FeS eutectic, to ~22 wt% in the case of anatexis up to 1300 °C (Singletary and Grove, 2003; assuming solid FeS was not exhausted in the source). The corresponding density range for 1200–1300 °C S-rich metallic melts is approximately 4200–5200 kg m^{-3} (Nagamori, 1969; Usselman, 1975; Kaiura and Toguri, 1979). Density for the picritic–ultramafic sort of silicate melt that could plausibly yield cumulates virtually devoid of plagioclase would be ~2800 kg m^{-3}. The solid ureilite silicates have 1200–

1300 °C densities consistently ~3200 kg m^{-3}. Together, these constraints imply that the metallic melt was ~1.3–1.6× denser than the solid mafic silicates and ~1.5–1.9× denser than the silicate melt; and solid FeNi was nearly twice as dense again as the metallic melt.

During the anatexis and percolation of silicate melt that must precede formation of a mainly melt magma chamber, the greater density of the metallic phase(s) would probably engender a major metal/silicate depletion. Even if by some fortuitous combination of circumstances the magma chamber nonetheless formed with a near-chondritic proportion of metal (S-rich melt?) to silicate (melt), before any final cumulate could form there would be strong potential for the dense metallic phase to concentrate into a relatively thin layer near the floor of the magma chamber. The individual cumulates would probably show enormous Ir diversity, much greater than the factor of ~5 observed among the proposed (Goodrich et al., 2004) possible cumulate ureilites.

As will be discussed in detail below, less ideally siderophile elements such as Au, Ni, As, Co, and Sb show highly systematic depletions relative to Ir in ureilites, and these depletion patterns probably reflect metallic melt vs. solid metal fractionations. If a minority of ureilites formed as cumulates but most formed as restites, it would be a remarkable outcome for both types to show similar metallic melt vs. solid metal fractionations. Yet LEW88774 and other augite-bearing or high-*mg* ureilites fall along the same Au, Ni, As, Co, and Sb depletion trends as all the other ureilites.

Siderophile constraints are not the only obstacle to a conventional cumulate model for ureilites. As noted by Clayton and Mayeda (1988), the gross oxygen-isotopic disequilibrium, including $\Delta^{17}O$, among ureilites indicates they were not derived from a single (or even a small number of) extensively molten silicate reservoirs.

Also, most ureilites have high proportions (average 3 wt%; review: Warren and Huber, 2006) of a carbon phase, graphite or "C-matrix," that has a density of 2200 kg m^{-3}. Several ureilites even have higher bulk-rock C than the most C-rich type of carbonaceous chondrite (CI, with 3.2 wt%: Wasson and Kallemeyn, 1988). In the case of RKPA80239, this is shown by multiple analyses of independently derived subsamples: Grady et al. (1985) found 5.5 wt% and Smith et al. (2001) 6.9 wt%. As solid mafic silicates and metallic phases accumulated in a negative-buoyancy relationship to their parent melt, graphite should have moved in the opposite direction. A few of the same augite-bearing ureilites that feature unusually low Ir (Fig. 1) do feature low bulk C. Hughes 009 has "no petrographically recognizable carbon phases" (Goodrich et al., 2001) and FRO90054 has only 0.24 wt% C (Grady and Pillinger, 1993). The normal-Ir augite-bearer META78008 is also relatively C-poor (1.5 wt%: Smith et al., 2001), but ALH82106/84136 has a C concentration (2.5 wt%: Jarosewich, 1990) very near the overall ureilite average.

Finally, mass balance implies that the putatively basaltic/picritic parent melts of cumulate ureilites should have also crystallized comparable volumes of Al-rich gabbroic or even anorthositic cumulates. Unless a magma ocean scenario is invoked (which would be grossly inconsistent with the survival of uniformly high siderophile concentrations in the ureilites), those Al-rich cumulates should have formed in proximity to the putative cumulate ureilites. The tiny smattering of feldspar-rich material in polymict ureilites has justifiably received a great deal of attention (Ikeda and Prinz, 2001; Goodrich et al., 2004; Kita et al., 2004). But as discussed above, bulk compositions of even polymict ureilites are still remarkably Al-poor. More than just traces of the complementary gabbro should be found, if a significant proportion of ureilites formed as cumulates from basaltic magma.

In summary, the siderophile and other constraints are clearly inconsistent with a conventional cumulate origin for ureilites. However, these constraints do not rule out some mild, localized form of the paracumulate scenario (Warren and Kallemeyn, 1989; Goodrich et al., 2004). Perhaps at times, within limited (augite-rich?) portions of an asteroidal-mantle restite, enough melt locally aggregated to induce a muted form of the efficient melt-displacement process (crystal accumulation) that gives cumulates their name. Basically, however, all ureilites appear to be restites.

5. Limited role of smelting

The term smelting refers to a simultaneous partial reduction and partial melting of rock. Thrush's (1968) industrial definition begins, "the chemical reduction of a metal from its ore by a process usually involving fusion." Most ureilites show obvious vestiges of what was, at least in a loose/arguable sense, an iron-smelting process. Their olivines feature distinctive reduced (FeO-depleted, Fe-metal sprinkled) rims (Singletary and Grove, 2003, reported quantitative estimates for the vol% reduced-rim in olivines of 20 ureilites). Yet all but the smallest olivines invariably retain cores that are, within any given ureilite, quite uniform in *mg*. The first-order classification of ureilites is typically based on olivine-core *mg*. Many authors (e.g., Goodrich, 1992; Goodrich et al., 2004; most expansively Singletary and Grove, 2003) have argued, or assumed, that the great diversity (Fo_{75-96}) of the ureilite mafic-silicate core compositions was engendered by varied degrees of smelting of a more uniform protoureilitic material. Warren (1996) argued that it is more plausible to simply assume that nebular processes produced an originally diverse suite of materials (as originally inferred from oxygen isotopes: Clayton and Mayeda, 1988), and the only major smelting was that which engendered the discrete metal-rich, FeO-poor rims. Recently, Mittlefehldt et al. (2005) have also argued for limited smelting. To distinguish the thoroughgoing (Singletary and Grove, 2003; Goodrich et al., 2004) type of smelting model from Warren's (1996) limited smelting model, we refer to the former as the smelted-cores model.

Before discussing the significance of siderophile elements vis-à-vis the smelted-cores model, we briefly note a related constraint first adduced by Warren (1996) and discussed in considerable detail by Warren and Huber (2006). The approximate temperature and pressure at which smelting could have occurred in the ureilites are well constrained: e.g., Singletary and Grove (2003) used olivine–pyroxene compositional relationships to derive a range of 1213–1301 °C for the equilibration temperature; and pressures implied by the observed range of olivine-core *mg* (75–96 mol%), assuming these *mg* reflect equilibrium smelting, have been constrained by thermodynamics (Warren and Kallemeyn, 1992) and experiments (Walker and Grove, 1993) to range from roughly 20 to 80 bars. The redox component of smelting

$$C + MgFeSiO_4 = MgSiO_3 + Fe + CO \quad (1)$$

implies that for every mole of $MgFeSiO_4$ (olivine) reduced, 1 mol of solid C must be consumed, and 1 mol each of $MgSiO_3$ (enstatitic pyroxene), Fe (metal), and CO (gas) must form. Eq. (1) indicates the proportions of materials in units of moles, but these can easily be translated into units of mass and even volume, by the general gas law, $PV = nRT$. The volume of 1 mol of CO gas at ~1200 °C and 80 bars, 1.5 L, dwarfs the combined volume of the reactants in Eq. (1). By stoichiometry-based mass balance (Warren and Huber, 2006), to shift *mg* from 75 to 96 mol% (the range of ureilite olivine-core *mg*) in an assemblage of (originally) ~75 wt% olivine implies formation of ~5.5 wt% CO gas. Even at 100 bars, the resultant volume proportion of CO gas (36 mol/kg) to rock (0.0003 m^3/kg) is 88 vol% gas, 12 vol% solid. Modifications for intermediate extents of olivine-core *mg* shift (yielding fewer moles of CO per kg of rock) or different lithostatic pressures involve simple application of the gas law. For example, keeping all other assumptions the same except $P = 20$ bars, the relative gas volume resulting from a 21-mol% *mg* shift is 97% of the product-mixture. Obviously, volume proportions of gas $\gg$ 10% could not be long sustained in any asteroidal interior.

It might be argued that the smelted-cores model is basically correct; it merely needs fine-tuning into a variant where smelting was not (as assumed by Singletary and Grove, 2003) an equilibrium process, but instead reduction proceeded with continual leakage of CO gas. A full discussion of the CO-leaky scenario is beyond the scope of this paper (cf. Warren and Huber, 2006). However, even supposing smelting occurred in a CO-leaky fashion, Eq. (1) still implies that for every gram of original FeO in olivine reduced, 0.78 g of Fe-metal must form. By stoichiometry, to shift *mg* from 75 to 96 mol% (the range of ureilite olivine-core *mg*) in an assemblage of originally ~75 wt% olivine implies production of ~11 wt% Fe-metal. Removal of silicate, roughly picritic partial melt at some stage of the smelting process might raise the restite's *mg* by a few mol% (Kita et al., 2004), but this still, in a scenario where smelting engenders the full range of ureilite olivine-core *mg*, implies production of ~8 wt% Fe-metal, not including Fe-metal formed in the later rim-reduction stage of smelting. No ureilite has been reported to contain as much as 8 wt% metal. If anything, available data (reviewed by Warren and Huber, 2006) indicate that ureilite Fe-metal abundance appears to anticorrelate with olivine-core *mg*. The highest reported metal abundances, 5–6 wt%, occur in two low-*mg* (Fo_{79}) samples, Goalpara and Haverö (Wiik, 1972). The ureilite with the highest olivine-core *mg*, ALH82106/4136, has only 0.5 wt% FeNi-metal (Jarosewich, 1990).

There remains one potential loophole for ureilite Fe-metal mass balance. In principle, as noted by Goodrich et al. (2004), most of the Fe-metal formed during smelting might have separated from the ureilites, possibly as solid Fe-metal but more plausibly as a component in S-rich metallic melt. The total Fe (Fe-metal plus Fe in FeS plus Fe in FeO) contents of ureilites are strongly anticorrelated with their olivine-core *mg* (Fig. 2). Hughes 009 and to a much lesser extent Dingo Pup Donga appear to represent exceptions, but both are severely weathered, and Hughes contains "no petrographically recognizable carbon phases" (Goodrich et al., 2001), so it is in any case an atypical ureilite.

The Fig. 2 trend is obviously inconsistent with any model in which smelting occurs without loss of Fe. Major Fe loss probably did not occur by FeO partitioning into the basaltic melts that separated from the ureilites. Melt/peridotite partitioning is not prone to engender major depletion in the FeO concentration of a restite. For example, application of the MELTS thermodynamical model to ureilites by Kita et al. (2004) resulted in restite FeO enrichment, with $D_{\text{resitite/melt}}$ for FeO ranging from 1.9 to 10.

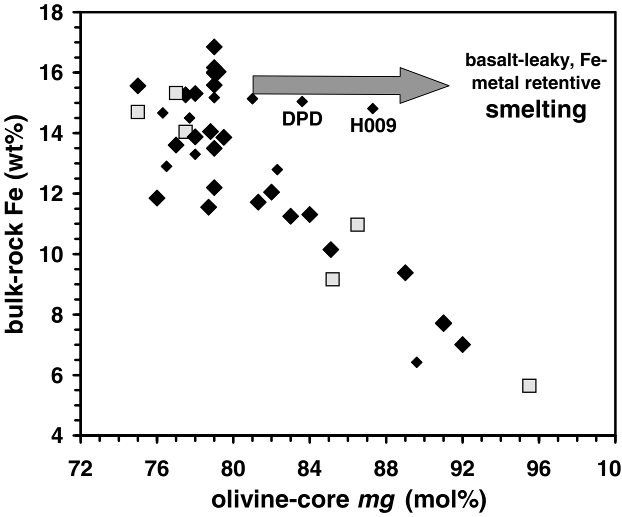

Fig. 2. Olivine-core *mg* vs. bulk-rock total Fe data for ureilites (*mg* data mainly from review by Goodrich, 1999; total Fe data from Table 2 and many literature sources, including those summarized in Table 3; cf. Fig. 1 of Mittlefehldt et al., 2005). Symbols have same meanings as in Fig. 1; darker symbols distinguish little-weathered ureilites from moderately to severely weathered warm-desert ureilites.

Loss of smelting-produced Fe-metal from the magnesian-core ureilites is also implausible, based on the siderophile evidence. If the high-core-*mg* ureilites lost especially large proportions of solid metal, these ureilites should feature strong depletions of highly siderophile elements, instead of the near-chondritic levels that we observe. In the case of Ir, the highest-*mg* ureilites do tend to have below-average concentrations, but only by a small factor (Fig. 1). Average Ir in 25 ureilites with olivine-core *mg* <82 mol% is 282 ± 153 ng/g; in 15 ureilites with *mg* ⩾82 mol% the average is 162 ± 54 ng/g, and the trend at high *mg* shows signs of converging near the Ir concentration of the highest-*mg* ureilite, ALH82106/4136, 157 ng/g (three analyses from two distinct pair-stones range from 149 to 163 ng/g: Spitz and Boynton, 1991; Warren and Kallemeyn, 1992). This level is still within a factor of 3 of the CI-chondritic value, so it would be implausible to appeal to loss of much more than 2/3 of the ~8 wt% of metal that according to the full-*mg*-range smelted-cores model should have formed. If the lost Fe^0-rich phase was mainly metallic melt, then chalcophile elements, i.e., S itself and elements with high distribution coefficient for S-rich metallic liquid over FeNi solid metal, $D_{ml/sm}$ (Chabot et al., 2003), should be most strongly depleted in the high-*mg* ureilites. Actual data for S (Fig. 3) and Ag ($D_{ml/sm}$ upwards of 100 for reasonably S-rich metallic melt compositions; nearly all data from Wang and Lipschutz, 1995; and Higuchi et al., 1976; see Table 3) show no correlation with olivine-core *mg*. Extensive data sets are also available (Table 3) for three elements that are strongly chalcophile, albeit no $D_{ml/sm}$ data are available: Zn, Cd, and In. Zinc (discussed in more detail below) is enigmatically high across the spectrum of ureilite types. The Cd and In distributions show enormous scatter, with essentially no correlation vs. Fo for In, but a marginally significant ($r = 0.48$ for 18 data-pairs) anticorrelation for Cd (Fig. 3). On balance, ignoring Zn, the available data seem permissive of considerable loss of S-rich metallic melt; possibly more from the high-*mg* ureilites than from low-*mg* ureilites, but not by large and systematic factors.

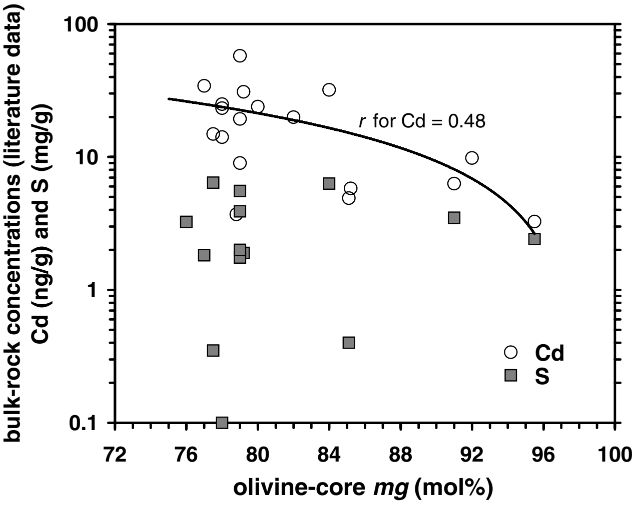

Fig. 3. Olivine-core *mg* vs. bulk-rock concentrations of chalcophile elements S and Cd in ureilites (literature data from many sources, for S most notably Jarosewich, 1990; nearly all Cd data from Wang and Lipschutz, 1995; and Higuchi et al., 1976; see Table 3). Cd shows a marginally significant anticorrelation with *mg*, but S itself shows no correlation.

Data for Ni and Au, elements that are strongly siderophile but also have $D_{ml/sm}$ (Chabot et al., 2003) close to 1, weigh against the magnesian-core ureilites having lost either solid Fe-metal or metallic melt to a much greater extent than ferroan-core ureilites. For Ni (Fig. 1b), the average in 27 ureilites with olivine-core *mg* <82 mol% is 1190 ± 440 µg/g; in 16 ureilites with *mg* ⩾82 mol% average Ni is 1160 ± 610 µg/g, and in ALH82106/4136 it is 1390 µg/g—above the overall average. Likewise, average Au in 26 ureilites with olivine-core *mg* <82 mol% is 25 ± 12 ng/g; in 15 ureilites with *mg* ⩾82 mol% it is 22 ± 10 ng/g, and in ALH82106/4136 it is 36 ng/g—1.5× the overall average. These relationships suggest that whatever Fe^0 loss occurred during ureilite petrogenesis was not especially extensive in the high-*mg* ureilites. Metal loss is not a plausible explanation for the failure of high-*mg* ureilites to contain abundant Fe-metal as implied by the smelted-cores model.

Summing up, the CO-gas volume problem alone should be enough to discredit the smelted-cores model. Even supposing that smelting might have occurred in a CO-leaky style (implying no buffering of mafic-silicate *mg*), there are problems with solid C (Warren and Huber (2006) and C isotopes (Hudon and Mittlefehldt, 2004) and also, as just discussed, with Fe-metal.

6. Ureilite siderophile depletion patterns

6.1. Siderophile depletion pattern characteristics

Ureilites, for a suite of igneous rocks, have a notorious reputation for capriciousness in their geochemistry. A significant correlation often seems hard to find. The ureilite siderophile depletions, however, show some highly systematic trends. Fig. 4a shows the correlation between Au and Ni. Discounting weathered samples, which appear, in many cases, to have lost Au and/or gained Ni, the scatter off the regression line is only what might be expected from a roughly 10–20% sampling "error" associated with typically ~300 mg samples, along with a few percent of additional analytical scatter. By the standards of strongly siderophile elements in igneous rocks, 10–20% as a typical sampling "error" is remarkably mild. Note that MET01085 falls near the regression line of the "normal" ureilites. Correlations for Au vs. Ir ($r = 0.61$) and Ni vs. Ir ($r = 0.64$) are not shown. But as the *r* values suggest, while clearly significant, the Au vs. Ir and Ni vs. Ir correlations involve far more scatter than Au vs. Ni. We doubt the higher scatter is analytical in origin. Evidently, the "noble" siderophile Ir is not hosted in the same phase(s) as the less "noble" Au and Ni.

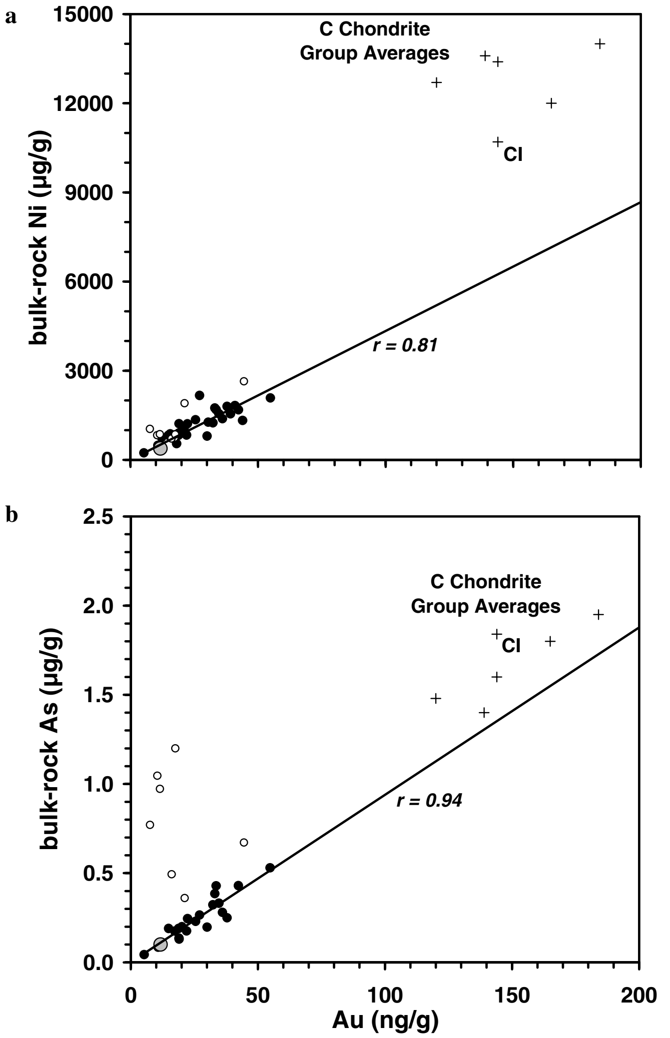

Fig. 4. Au vs. (a) Ni and (b) As in ureilites (Tables 2 and 3). Among ureilites (circles), open symbols denote weathered warm-desert samples. Large, gray-filled symbol denotes MET01085 (which contains no olivine). Shown for comparison (crosses) are group-average concentrations for carbonaceous chondrites (Wasson and Kallemeyn, 1988; Kallemeyn et al., 1994).

A tighter correlation is manifested if instead of simply Au vs. Ni we plot Au/Ir vs. Ni/Ir (Fig. 5a). Co/Ir, Sb/Ir, and especially As/Ir also show good correlations vs. Au/Ir (Figs. 5b–d). Similar correlations for Au/Ir vs. Se/Ir ($r = 0.82$) and Te/Ir ($r = 0.89$; using entirely literature data for Te) are not shown. Similar but weaker correlations (not shown) are found if against these same ratios Ni/Ir is plotted instead of Au/Ir. Note that each of these Au/Ir-correlated depletion trends tends to roughly parallel a similar trend among the carbonaceous chondrites; a point to which we will return later.

In Fig. 5, most ureilites cluster toward the low Au/Ir ends of the trends; with Co/Ir, As/Ir and especially Ni/Ir much lower than the carbonaceous–chondritic ratios. One might suspect that the samples with the highest Au/Ir and Ni/Ir could be petrologically unusual. However, the three samples with the highest Au/Ir, Y-790981, ALHA81101, and LEW85328, are mineralogically nondescript olivine–pigeonite ureilites. Texturally, ALHA81101 is mosaicized, but LEW85328 and Y-790981 are “typical” (Mittlefehldt et al., 1998). One unusual circumstance is that for both LEW85328 and Y-790981 the only Ir data are from Spitz (1992) while the only Au data are from Wang and Lipschutz (1995). However, the Au/Ir ratios are probably accurate, because these two samples fall close to overall correlations on plots of Au/Ir vs. Sb/Ir (Fig. 5d) and Se/Ir, based on Sb and Se data also from Wang and Lipschutz (1995). The composition for ALHA81101 is an average of very similar results from four analyses: two by Warren and Kallemeyn (1992), one by Spitz and Boynton (1991), and one by Wang and Lipschutz (1995).

Compared to the systematic trends shown by siderophile elements in ureilites, the siderophile distributions in lodranites, which are probably also asteroidal mantle restites (but from lower degrees of partial melting), are more scattered and commonly feature Au/Ir, Ni/Ir, etc., much greater than chondritic (review: Mittlefehldt et al., 1998). For example, CI-normalized Au/Ir ranges from 0.5 to 2.1, and CI-normalized Ni/Ir from 0.3 to 3.0, among just 8 lodranites with available data. The average lodranite Ni concentration is about 13,000 µg/g, or ~11× the average for ureilites.

The more extremely siderophile elements, such as Os, Ru and, at low fO_2, Re, appear to remain, among bulk-ureilite compositions, in nearly chondritic proportion to Ir. For example, the strong correlation between Os and Ir (not shown; $r = 0.97$) has a slope implying $\text{Os/Ir} = 1.2$; among various types of chondrites this ratio is uniformly 1.1 (Wasson and Kallemeyn, 1988). Osmium isotopic data (Rankenburg et al., 2005) also indicate minimal fractionation between Re and Os during ureilite petrogenesis. The main host phase for strongly siderophile elements is probably minor Ni-poor FeNi metal (kamacite, with typically 3–7 wt% Ni: Berkley and Jones, 1982; Janssens et al., 1987; Mittlefehldt et al., 1998). The kamacite occurs mainly as highly elongate grains of order 0.1–1 mm long, interstitial to the mafic silicates (i.e., in the intergranular space sometimes described as a system of “veins,” and otherwise filled with “C-matrix” carbon phases), but also, in the most texturally pristine, unmetamorphosed and unbrecciated, ureilites, as portions of metal + sulfide spherules within silicate grains (Berkley and Jones, 1982). In addition, and not to be confused with the intergranular gains that host most of the Ir, Ni, etc., there are tiny, extremely Ni-poor metals scattered throughout the reduced silicate rims.

6.2. Potential mechanisms for origin of siderophile depletion patterns

There appear to be basically two potential mechanisms for engendering systematically diverse siderophile-element concentrations in primitive achondrites such as the ureilites. One obvious potential mechanism is metal/silicate

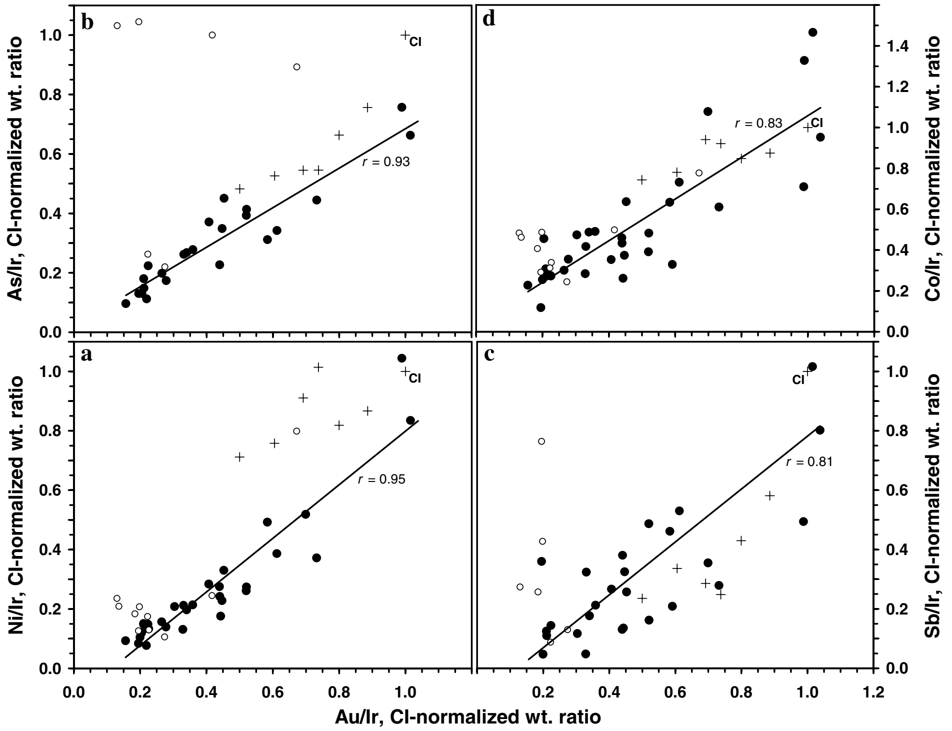

Fig. 5. Au/Ir vs. (a) Ni/Ir, (b) As/Ir, (c) Sb/Ir, and (d) Co/Ir in ureilites (Tables 2 and 3). Symbols have same meanings as in Fig. 4. Open symbols denote weathered warm-desert samples. Shown for comparison (crosses) are group-average concentrations for carbonaceous chondrites (Wasson and Kallemeyn, 1988; Kallemeyn et al., 1994).

fractionation, including metallic-melt/silicate fractionation, such as might occur in the process of core formation. The other potential mechanism for engendering systematic siderophile-element diversity might be volatility-linked fractionation, such as during condensation, evaporation and/or sublimation of the parent materials while still in small, unmelted bodies interacting with the solar nebula gas. Chondrites, which are in essence products of volatility-linked (but also strongly grain-size influenced, and thus complex) fractionation of the bulk solar system, have diverse siderophile-element patterns (at least in terms of some of the less "noble" siderophile elements: Walter et al., 2000), and there is little reason to assume that the most volatile- and C-rich type of chondrite (CI) is highly representative, in this sense, of the parental materials of the ureilites.

Much of our discussion of these alternatives will be couched in terms of the average composition of all ureilites (Table 3). We find little basis for distinguishing subclasses of ureilites vis-à-vis siderophile geochemistry; they appear to represent a compositional continuum.

Olivine-core *mg* has been very widely used, since Berkley et al. (1980), as a basis for petrologic subclassification of ureilites. However, among ureilites, olivine-core *mg* is strongly anticorrelated with $\Delta^{17}O$, the diversity of which is undoubtedly of nebular, not igneous origin (Clayton and Mayeda, 1988; Franchi et al., 1998); and products of nebular processes (chondrites) do not feature major *mg*-linked siderophile variations. In any event, the systematic ureilite siderophile depletions show only loose or nonexistent correlation with olivine-core *mg*, or for that matter with other petrologic parameters conventionally used for classification. The highest-*mg* ureilites tend to have below-average Ir, but many low-*mg* ureilites are similarly Ir-poor; and the lowest Ir levels occur in a trio of Fo_{79-80} ureilites (Fig. 1). A similarly loose, at best, correlation with presence of augite has already been discussed, in connection with the cumulate hypothesis. As discussed above, in terms of Au/Ir, the relationship with olivine-core *mg* appears to be near-random scatter.

6.3. Inheritance of volatility-linked nebular fractionations?

Fig. 6 shows the average ureilite composition (Table 3) ordered by element volatility, as measured by the thermodynamically calculated temperatures for 50% condensation in a solar-nebula setting (Wasson, 1985), for a wide variety of elements that range from highly siderophile (Ir-like; e.g., Os, Re, and Ru) to moderately siderophile (Ni, Ge, As, and Sb) to chalcophile (e.g., Zn, Se, Cd, In, Te, Tl, Bi, and Pb). Our reason for also including C will be explained shortly. To illustrate on an element-by-element basis the importance of avoiding weathered samples, two variants of the average ureilite composition are plotted. The version including highly weathered samples shows major enrichments in some elements, particularly As, Sb, Br, Bi, and Tl. Obviously, only the little-weathered data set should be used for petrogenetic modeling. However, for most

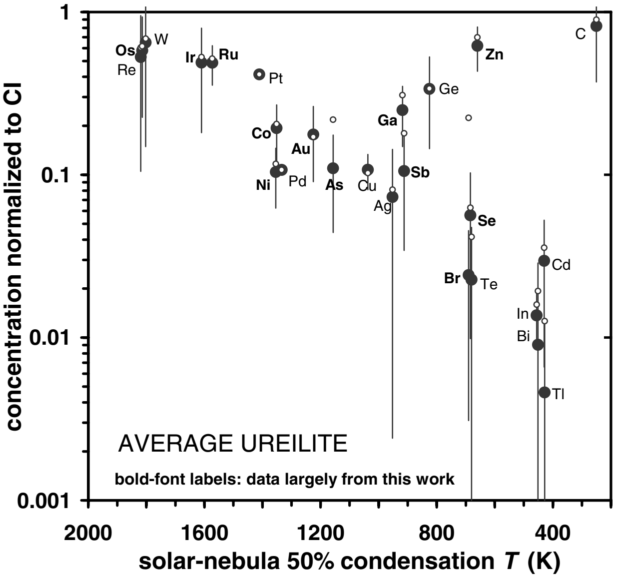

Fig. 6. Average ureilite composition (Table 3) shown as a function of thermodynamically estimated temperatures for 50% condensation in a solar-nebular setting (Wasson, 1985). Larger, filled symbols (with 1-σ error bars) are based on data set restricted to little-weathered samples; open symbols are based on all ureilites. Note that for some elements, e.g., As and Br, elimination of weathered samples is essential to avoid major errors in the average composition.

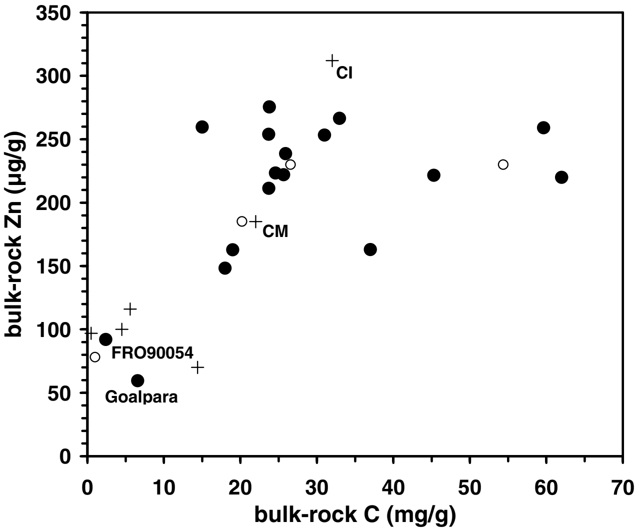

Fig. 7. In common with group-averaged carbonaceous chondrites, ureilites show a loose positive correlation between bulk-rock concentrations of C and Zn (mostly literature data; for chondrites mostly from Wasson and Kallemeyn, 1988; and Jarosewich, 1990). *Note.* Ureilite plotted at 1 mg/g C is Hughes 009; no actual C measurement is available, but the meteorite appears devoid of C phases (Goodrich et al., 2001).

elements the effect of including weathered samples would hardly be noticeable.

The depletion pattern in Fig. 6 is not highly systematic. However, there is a tendency for volatile elements to be more depleted than refractory elements. Among the trace elements (i.e., excluding C), the only major exceptions to this tendency are Ge and especially Zn. In the case of Zn, it seems conceivable that the mildness of the depletion stems from linkage to a C-phase (graphite?) at some early stage in the evolution of the parent material. Obviously, and anomalously, C was not much depleted in ureilites. Most of the more volatile elements plotted in Fig. 6 show, among ureilites, no correlation whatsoever with C. However, Zn shows a loose but statistically significant correlation with C among ureilites, and also among carbonaceous chondrites (Fig. 7). For ureilites ($r = 0.59$), this correlation might be to a slight extent artificially weakened by compilation of the data entirely from separate and unrelated C and Zn analyses. Unfortunately, we know of no data that would confirm or refute our speculation that Zn was linked, during a process that otherwise engendered volatility-linked fractionations, with C. In one of the few ureilites that bears Cr-spinel, a major fraction, probably at least half, of the total Zn appears to reside in Cr-spinel, according to *e*-probe data from Chikami et al. (1997; compared with bulk-rock Zn from this work). As a divalent transition element, Zn is probably also moderately compatible with mafic silicates. Janssens et al. (1987) found that a nearly pure C-matrix (or "vein") subsample of Haverö is very Zn-poor (5.5 μg/g) compared to the bulk rock (~160 μg/g). However, the phase hosting Zn is not necessarily the same now (post-anatexis), as earlier, when chondritic/nebular fractionations occurred. As for Ge, there are too few data for ureilites to meaningfully test for a correlation between Ge and C. But the 6 data-pairs that are available manifest a loose ($r = 0.60$) correlation.

Evidence for nebular (or anyway, pre-igneous) fractionation comes from the parallelism between the various Au/Ir-correlated depletion trends (Ni/Ir, As/Ir, Co/Ir, and Sb/Ir) and similar trends among the carbonaceous chondrites (Fig. 5). The chondritic trends are presumably nebular in origin. Elements such as Au, As, and Sb are somewhat "labile," so conceivably chondritic parent-body alteration processes to a large degree redistributed them. But if such redistributions could easily overprint nebular compositional trends, then the final Au/Ir (etc.) ratios would probably be far less systematic (Wasson and Kallemeyn, 1988; Xiao and Lipschutz, 1993; Kallemeyn et al., 1994) among different individual chondrites and chondrite types. The mechanism(s) by which nebular processing might have engendered correlations involving Au/Ir with Ni/Ir, As/Ir., etc., is beyond the scope of this paper. However, among the chondrite types, these ratios tend to correlate with bulk S abundance (Fig. 8). In the nebular setting, sulfur's outstanding trait was volatility. Its 50% condensation *T* (Wasson, 1985) is similar to those of Zn and Se.

6.4. An "incomplete" variety of core formation?

Core formation is sometimes thought of as involving mainly metal (FeNi), with S only playing a secondary, non-essential role. In the case of the ureilites, the limited extent of core formation may have involved only a subordinate role for FeNi-metal. As indicated in Fig. 9, both Fe

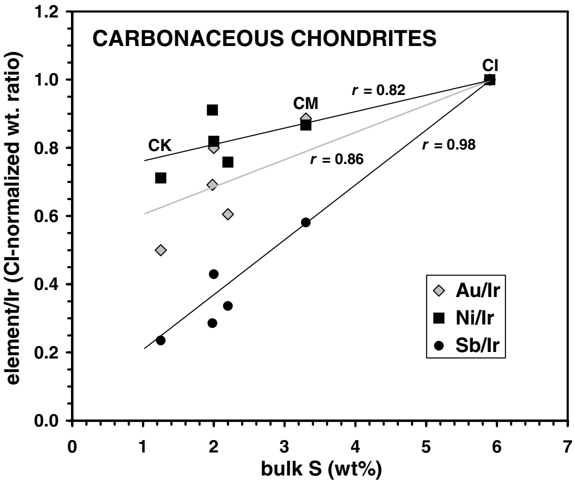

Fig. 8. Au/Ir, Ni/Ir, and Sb/Ir all show positive correlations with S among group-averaged carbonaceous chondrites (data sources as for Fig. 7). Trends (not shown) for Co/Ir and As/Ir are very similar to plotted trends for Ni/Ir and Au/Ir, respectively.

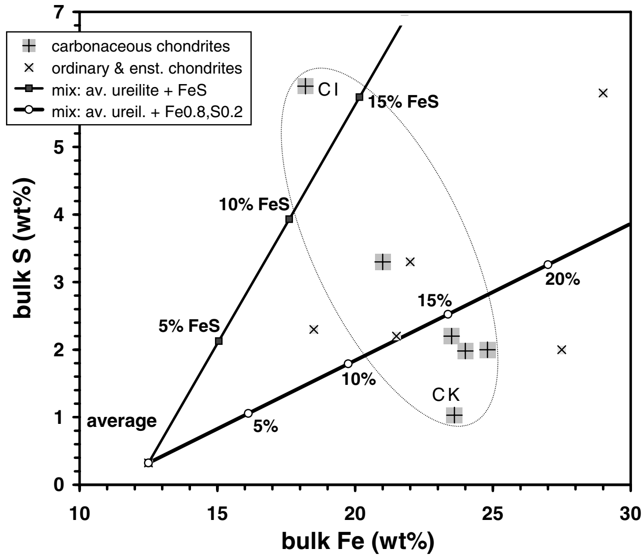

Fig. 9. Bulk Fe vs. S for group-averaged chondritic meteorites (Wasson and Kallemeyn, 1988; Jarosewich, 1990), also showing potential mixing proportions between average ureilite (Table 3) and stoichiometric FeS or a 15 wt% S metallic melt.

and S are depleted in ureilites in comparison to carbonaceous chondrites. The depletion factor for S is highly uncertain, because the carbonaceous chondrites span a very wide range. However, the most S-poor carbonaceous chondrite types tend to also be C-poor; CK has just 0.3 wt% C, and thus is totally unsuitable as ureilite parental material (Jarosewich, 1990). Excluding CK, the average ureilite is depleted in S relative to all other chondrite types by factors of 6–18. Sulfur is uncommonly volatile, so conceivably the missing S was entirely lost prior to the assembly of the ureilite parent asteroid(s). But the accompanying major depletion in Fe, which is not volatile, suggests that a major proportion of S, presumably as S-rich metallic melt, was lost through parent-body processing.

A plot analogous to Fig. 6 but with low-pressure metal/silicate distribution coefficient $D_{m/s}$ in place of 50% condensation T would not yield a systematic pattern. As reviewed by Walter et al. (2000), $D_{m/s}$ is much higher (more Ir-like) for Au and Ni than for some elements (Ga, Co) that are less depleted than Ni and Au in the average ureilite composition. In any case, $D_{m/s}$ is extremely high for elements showing only mild depletion in the average ureilite composition (e.g., Re, Os, and Ir) and lower, but still much greater than 1, for elements showing larger depletions (Cu, As, and Ag). Thus, any process that enhanced the FeNi/silicate ratio in the ureilites should have enriched, not depleted, all of these elements, but any process that diminished the FeNi/silicate ratio should have depleted Re, Os and Ir far more than Cu, As, and Ag. It seems safe to conclude that the ureilite siderophile patterns were not determined by fractionation of FeNi metal from silicate.

Fig. 10 again shows the average ureilite composition (Table 3), this time ordered by the element's distribution coefficient for S-rich metallic liquid over FeNi solid metal, $D_{ml/sm}$, as constrained experimentally by Chabot and Jones (2003) and Chabot et al. (2003); cf. Righter (2003). The most appropriate composition for a putative ureilitic metallic liquid is admittedly difficult to constrain. For Fig. 10, we have assumed 22 wt% S, along with 3.6 wt% Ni (i.e., a chondritic Ni:Fe proportionality of 0.05) and 1 wt% each of C and P. This S content was chosen because the phase equilibria of the Fe–FeS system (Usselman, 1975; Fei et al., 1997) suggest 22 wt% is a plausible composition in the case of anatexis at ~1250 °C (Singletary and Grove, 2003); even higher S, up to 31 wt% at the FeS eutectic, might be expected for the earliest stages of anatexis.

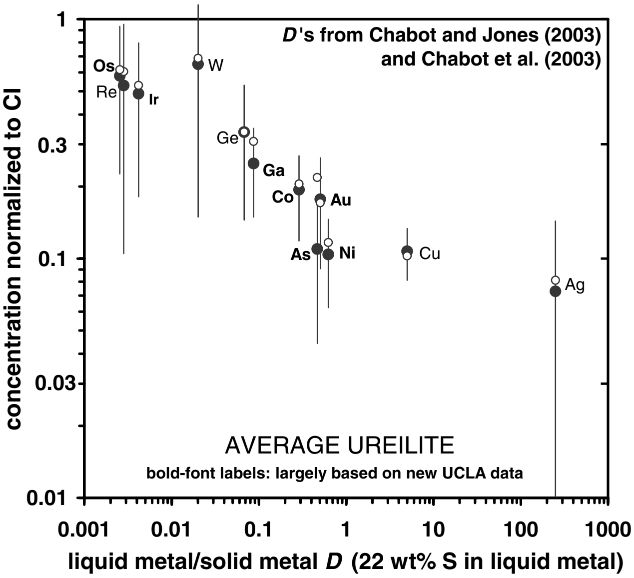

Fig. 10. Average ureilite composition (Table 3) shown as a function of $D_{ml/sm}$ (Chabot and Jones, 2003; Chabot et al., 2003). Larger, filled symbols (with 1-σ error bars) are based on data set restricted to little-weathered samples; open symbols are based on all ureilites. Note that for As, elimination of weathered samples is essential to avoid major error in the average composition.

The ureilite depletion pattern appears more smooth and orderly in Fig. 10 than it does in Fig. 6. However, the smoothness of fit in Fig. 10 may be largely artificial. No $D_{ml/sm}$ is yet available for Zn, the element that is fit worst, apart from C, in Fig. 6. As a chalcophile (but also largely lithophile) element, Zn is likely to have a high $D_{ml/sm}$. As a further caveat, the assumption that the metallic melt contained 1 wt% C is extremely uncertain. Spherules found as rare inclusions in some ureilite mafic silicates have more C (~4.1 wt%) than S (~2.9 wt%) (Goodrich and Berkley, 1986). The potential effects of C on $D_{ml/sm}$ are still poorly understood, but recent preliminary experiments (Chabot et al., 2006) suggest that C may have important effects on W and Re.

Assuming the greater smoothness of the Fig. 10 trend in comparison to the Fig. 6 trend is truly significant, a model of depletion by fractionation between S-rich metallic liquid and solid metal, as in the early stages of core formation, would appear to be favored over a model of volatility-linked fractionation. Goodrich et al. (1987) long ago envisaged a major role for $D_{ml/sm}$-linked fractionations in ureilite petrogenesis, but within the context of a complex model in which the ureilites formed as cumulates, and their parent melts were derived by remelting of earlier crustal mafic cumulates that were at high enough fO_2 to not be saturated with Fe-metal.

A variant of the diagram in Fig. 10, but assuming much lower S in the metallic melt, say 5 wt%, would look qualitatively similar, except with greater apparent scatter. The median $D_{ml/sm}$ would again be close to 1. However, the total $D_{ml/sm}$ range (Os to Ag) would only be from 0.2 to 10 (Chabot and Jones, 2003; Chabot et al., 2003; cf. Rushmer et al., 2004). For many of the elements with major depletions in ureilites (prime example: Ni), $D_{ml/sm}$ would be very close to 1. Clearly, the metallic liquid must be S-rich to have any potential for engendering, by separation from solid FeNi, the great range of depletion factors characteristic of even the average ureilite siderophile depletion pattern.

6.5. Some combination of the two mechanisms

Fig. 4 shows Au vs. Ni and vs. As for ureilites along with carbonaceous chondrites. On Fig. 4b, the ureilite and carbonaceous chondrite trends point in the general direction of each other. At first glance, the evidence again suggests that the ureilite depletions of moderately siderophile elements may stem from mainly nebular (volatility-linked?) fractionations. However, the well-defined slope of the ureilite Au vs. Ni trend (Fig. 4a) extrapolates significantly to the low-Ni/Au side of the compositional range of carbonaceous chondrites. This implies (or rather confirms) that the siderophile fractionations among ureilites are at least partially the result of a secondary, non-nebular process, i.e., removal of S-rich metallic melt.

Large depletions in Fe relative to carbonaceous chondrites suggest that a fairly large proportion of S-rich metallic melt was probably lost from the parental material. The most Fe-rich ureilite, Goalpara, contains 16.9 wt% Fe; most contain <15 wt% (Fig. 2). Evolution to the average ureilite composition starting from the range of carbonaceous chondrites would imply removal of at least 10 wt% of S-rich metallic melt (Fig. 9). If this mechanism is assumed to also account for the entire spread in bulk Fe between low-*mg* and high-*mg* ureilites (Fig. 2), the implied metallic melt loss for the highest-*mg* ureilites would reach ~20 wt%. As discussed above (Fig. 3), consistent with such a model the chalcophile Cd shows a loose, marginally significant anticorrelation with olivine-core *mg*, but neither S nor the high-$D_{ml/sm}$ element Ag, nor Zn nor In, shows any significant anticorrelation.

The refractory elements Os, Re, Ir, and Ru provide evidence against volatility as the principal cause of the ureilite siderophile depletions. Although the depletions for these highly siderophile elements are relatively mild (Figs. 1 and 10), their ureilite-average concentrations are still below the levels in any known type of chondrite (and this, despite the loss of roughly 1/5 of the original material as a basalt component). In some ureilites, e.g., ALHA81101 (Warren and Kallemeyn, 1992), these Ir-like elements are depleted by factors of ~10. These depletions, albeit by igneous-rock standards comparatively mild, cannot plausibly be attributed to volatility. They also cannot be attributed to fractionation of S-rich metallic melt (Fig. 9). They probably developed when only minor proportions of solid FeNi-metal were present to compete for Ir with down-percolating metallic melts that were relatively S-poor (perhaps as a result of prior metallic melt removal), and thus had relatively moderate $D_{ml/sm}$ (Chabot and Jones, 2003). Conceivably, the Ir depletions also developed largely as a result of entrainment of fine-grained FeNi-metal as S-rich metallic melts oozed out of the restites. Most of the (relatively) Ni-rich metal in ureilites occurs as large (of order 0.1–1 mm), elongate grains that would not easily be entrained with out-flowing melt. However, Wlotzka (1972) described a component of "very small (~1 μm and less)" grains of "apparently" Ni-rich metal occurring within "black vein" areas (i.e., not within the reduced silicate rims) of Haverö. The FeNi-entrainment hypothesis would imply that such grains are only the surviving remnant of what was once a larger population of small, Ni-rich grains.

On balance, the available evidence favors fractionation of S-rich metallic melt as the predominant factor that engendered the ureilite siderophile patterns; with inherited solar-nebular fractionations (especially for Zn?) and fractionation of minor FeNi-metal as secondary factors. We can also infer that FeNi-metal was probably never a major phase in the protoureilites. The average ureilite has Ni/Ir depleted to 0.21× CI (or 0.23–0.29× other common types of carbonaceous chondrites). Yet the experimental data of Chabot and Jones (2003) indicate that $D_{ml/sm}$ is negligibly small for Ir, and for Ni can never be $\gg$1.0 (even assuming exotic C and/or P concentrations in the S-rich metallic melt). Thus (conservatively ignoring the likelihood that Ni/Ir fractionation was dampened by inefficient separation of metallic melt from FeNi-metal), the 3- to 5-fold depletion in Ni/Ir suggests that before the metallic melt separated from the ureilites, the mass ratio of metallic melt to solid FeNi was at least 3.

7. Melt percolation and core formation during ureilite anatexis

7.1. Melt porosity: a key issue

Initiation of core formation, i.e., the first downward percolation of metallic melt (Fe–S, or, in principle, Fe-metal), is probably triggered when the anatectic melt fraction (porosity) within the mantle reaches some threshold value for melt connectivity. Metallic melt probably starts forming at the Fe–FeS eutectic, ~990 °C (Usselman, 1975), well below the temperature where significant silicate melt would form. Experimentally constrained solidi for chondrites, including Allende (CV), Murchison (CM) and two ordinary chondrites, are consistently close to 1150 °C (Jurewicz et al., 1995). However, as discussed by, e.g., Rushmer et al. (2000), the high dihedral angle of metallic melts with mafic silicates suggests that connectivity, and thus melt percolation, may not commence until the silicate melt fraction *f* is quite large.

Just how large *f* must become to enable core formation is highly uncertain. Experiments by Lebedev et al. (1999) led these authors to estimate that an *f* of 5–10 vol% is probably required to enable percolation of S-rich metallic melt. However, Herpfer and Larimer (1993) reported experimental results implying that 1–2 vol% of melt (whether this meant silicate melt or combined silicate + metallic melts, is not clear) would suffice. In contrast, Yoshino et al. (2004) inferred from their experiments that very small proportions of silicate melt actually inhibit the connectivity of molten Fe–S. They estimated that the percolation threshold of Fe–S melt in the presence of moderate degrees (roughly 20–25 vol%) of silicate melt at 1-*g* is 13 ± 2 vol.%; i.e., they found that even when percolation commences, ~13 vol% of Fe–S melt remains stationary (“trapped” in the solid silicate matrix; cf. Walker and Agee, 1988). Yoshino et al. (2004) also argued that efficient removal of residual Fe-metal (~5 vol.%) from peridotitic silicate requires considerably higher-degree melting of the peridotite “so that the metal can segregate as droplets.”

Numerous authors (Ikeda and Prinz, 2001; Goodrich et al., 2004; Kita et al., 2004) have recently suggested that ureilite partial melting was fractional, implying the melt fraction *f* was near zero throughout the melting and melt-extraction process. Ikeda and Prinz (2001) argued that the melting style was fractional based upon evidence from Goodrich’s (1999) MELTS-based study, which indicated that batch partial melting of an alkali-rich (CI) type of chondritic source would yield orthopyroxene, not pigeonite, as the main restitic pyroxene, whereas (these authors supposed) fractional melting, by depleting the alkalis at low aggregate *f*, would eventually yield abundant restite pigeonite. Ikeda and Prinz (2001) also argued that fractional melting is best suited to explain the typically alkali-depleted nature of rare feldspathic clasts within polymict ureilites. Goodrich et al. (2004) added that fractional melting seems better suited to preserve the great heterogeneity of O-isotopic ratios (Clayton and Mayeda, 1988) among ureilites. Kita et al. (2004) added that the rare feldspathic clasts within polymict ureilites are typically depleted in not only alkalis but incompatible elements in general.

An ideally fractional style of anatexis would imply that *f* never reached even the lower end (1–2 vol%) of the range that physicists (Herpfer and Larimer, 1993; Lebedev et al., 1999; Yoshino et al., 2004) believe would be required to trigger the metallic melt percolation process, i.e., core formation. In experiments specifically designed to constrain ureilite petrogenesis, Walker and Agee (1988) noted that during melting of an Allende (CV) composition, S-rich metallic melts show a remarkable tendency to remain immobile, “fixed” with residual olivines, even as fairly large proportions of silicate melt (~25 vol%) form and percolate apart from the residual olivines. Walker and Agee (1988) inferred from the extensive depletion of sulfur from the ureilites that a large proportion of silicate melt was present at some stage of their anatexis. We infer above that metallic melt percolation was sufficiently vigorous to entrain enough FeNi-metal to engender mild but significant depletions of Ir-like elements in the ureilites. The siderophile/sulfur evidence thus seems to militate against fractional melting (or even near-fractional melting) as the prevailing style of ureilite anatexis. Conversely, if the mainly fractional melting model is correct, we may need to reexamine some of our inferences about the origin of the ureilite siderophile depletions.

7.2. Fractional melting?

MELTS calculations by Kita et al. (2004) show that provided the parent material is assumed to resemble (in terms of compositional traits such as alkali, Al and Ca abundances) CM rather than CI carbonaceous chondrites, there is no need to invoke extraordinary alkali-depletion to account for pigeonite as the dominant restite pyroxene. There is little reason to assume that CI is a closer match than CM, for such traits, to the parental material. In terms of O-isotopes (Clayton and Mayeda, 1988), CI appears the least suitable type of carbonaceous chondrite. CI has the highest C abundance, but CM is 0.69× as carbon-rich as CI.

There is no reason to be confident that the polymict ureilites’ tiny component of feldspathic matter is representative of the overall melt products from the parent asteroid(s). In the explosive volcanism basalt-loss scenario, which even some partisans of fractional partial melting endorse (Goodrich et al., 2004), the blown-off basalt mostly never re-accreted to the parent asteroid. The tiny fraction that did manage to survive (avoid blow-off or else re-accrete) probably was not simply random. It probably survived, where almost all the rest did not, for some reason. It seems possible, if not likely, that the surviving basaltic component is dominantly material that erupted late compared to most of the rest of the basalt. If so, it represents the last dregs of melt that formed and remained within the restite. As suggested by several authors (e.g., Warren and Kallemeyn, 1992; Goodrich et al., 2004), the ureilites probably acquired their "frozen-in" high equilibration temperatures (1210–1300 °C: Singletary and Grove, 2003; cf. Takeda et al., 1989) because the parent asteroid(s), while still hot and anatectic, suffered a catastrophic disruption. The last melt out, in this scenario, may have come from material that had such low-φ (local melt porosity) that the melt would never have managed to out-percolate, under normal circumstances. Purging of extreme low-φ restites was probably facilitated by the catastrophic disruption of the parent body(ies). Distances to space (i.e., the surface) were suddenly diminished and thermal gradients were suddenly enhanced. In consequence, purgation of melt must have been enhanced by the thermal-driving mechanism of Walker and Agee (1988). Also, the CO-leaky, rim-reducing form of smelting was jump-started by sudden pressure drop (the smelting reaction is extremely *P*-sensitive), implying abundant CO gas outflow, which would have facilitated out-migration of melt. The jetting out of CO gas probably prolonged the reassembly of the asteroid, and may well have caused the initial fragments to continue to disintegrate, as diminution of pressure caused "runaway" olivine-rim smelting, until the residual fragments were so small, melt-purged and fast-cooling that the process finally turned itself off. On the other hand, the lower and lower pressures within the interiors of the break-up fragments would have translated into relatively low velocities for the (gas-expansion-driven) explosive volcanism (cf. Goodrich et al., 2004); the last-dreg basalt eruptions would thus have been propelled to only short distances from the parent break-up fragment, and might therefore have been more prone than earlier blow-out matter to remain within the gravitational well of the overall (temporarily, pending reassembly, diffuse) parent asteroid. All or some of these factors may have caused the last-erupted basalts to come from regions where tiny dregs of melt managed to form/survive in regions that had previously been extensively melted and extensively purged; i.e., source regions that might have been severely depleted by prior cycles of "normal," moderate-φ melting.

In any event, the scarce feldspars observed in monomict ureilites (samples that have probably undergone considerable anatexis—enough to nearly eliminate their original chondritic complements of feldspar and Al) are not alkali-poor. These survivors are An_{22} in FRO90168 (Bland, 1993) and mostly $An_{<23}$ in EET96001 (Warren et al., 2006). Also, NWA766 (this work) contains a 50×10 μm grain of high-Al glass with near-feldspar (albeit "ternary") stoichiometry; and this glass, calculated as feldspar, is An_6Or_7 (the grain is transected by an Fe-rich weathering vein, so the analysis may be impure; major oxides in wt% are SiO_2 73.3, Al_2O_3 14.8, Na_2O 6.1, FeO 1.2, K_2O 0.80, CaO 0.74, and TiO_2 0.39, MgO 0.35).

Survival of O-isotopic heterogeneity is a powerful argument against extensive melting, but in an asteroidal environment of low *g* and limited thermal longevity, "extensive" should be understood to imply that melting has engendered such a high melt-porosity that the bulk material, or at least an interstitial melt component, can undergo convective (or other) stirring. In the low-*g* asteroidal environment, the melt-porosity threshold for convection probably implies either a magma, i.e., a partial melt that (with perhaps minor suspended crystals) that has *separated* from its restite source; or else an anatectic zone at very high (above perhaps 20%?) melt fraction. Without fluid stirring, diffusive mixing alone, even at a magmatic temperature (say 1300 °C), will not homogenize even a molten basaltic material (in $<10^9$ years) over length-scales much greater than 0.5 km (Warren and Kallemeyn, 1992; Scott et al., 1993). Moreover, there is no guarantee that all of the diverse ureilites derive from a single asteroid.

7.3. Percolation theory

In this section, we use melt percolation theory to constrain *f* during the anatexis that produced the ureilites. The near-total removal of basalt from the ureilites implies that a large proportion of silicate melt was removed by the end of anatexis. From mass balance, a lower limit of 13 wt% is implied for the aggregate proportion of removed basalt, assuming that the starting chondritic material had at least 1.1 wt% Al (the most Al-poor known type of chondrite, CI, adjusted to anhydrous composition), that the basalt had no more than ~6.5 wt% (cf. an average eucrite or VLT lunar basalt), and that the average final ureilite has ~0.30 wt% (see above). If we assume more realistically that the starting material had an Al content similar to the average of the six main types of carbonaceous chondrite (CI, CM, CO, CV, CK, and CR, adjusted to anhydrous), 1.5 wt% (Wasson and Kallemeyn, 1988; Jarosewich, 1990), the lower limit for aggregate basalt removal would increase to 21 wt%.

Percolation-compaction theory (McKenzie, 1989) suggests that if the final φ is required (by the dearth of residual plagioclase and Al) to be very low, say 1%, and the source region's φ during anatexis is assumed to never reach a large fraction of the aggregate proportion of melt removed, then the out-percolation process would be prohibitively slow. The relative velocity of melt (vs. solid matrix) ω is given by

$$\omega = k(1-\varphi)\Delta\rho g/(\mu\varphi), \tag{2}$$

where k is the permeability of the matrix, φ is the total melt porosity (which we will assume is approximately the same as a "batch" silicate *f*, although some additional melt porosity was probably present in the form of immiscible metallic melt), $\Delta\rho$ is the solid-melt density disparity, and μ is the melt viscosity. h is the thickness of the mush layer, and g is the local gravity. At small φ, the time required for percolation to lower the melt fraction by a factor $1/e$ is

$$t_p = \varphi h\mu/(k\Delta\rho g), \tag{3}$$

where h is the thickness of the mush layer, and g is the local gravity. If h is the whole-mantle thickness of a small body such as an asteroid, g is approximately proportional to h; i.e., t_p is insensitive to the assumed size of the asteroid. The melt viscosity, assuming a eucrite-like composition, is estimated (method of Shaw, 1972) to be ~10 Pa s. We use the model of Wark and Watson (1998) for k as a function of grain size (assumed radius, 1 mm) and φ. Typical results, for $\varphi = 1$–10%, are 2×10^{-14} to 4.5×10^{-11} m^2. As an example of the quantitative implications of Eq. (3), the calculated time for out-percolation of melt from an initial φ of 20% to a final φ of 1% is 21 Ma. But if we assume that instead the same total melt removal (19%) is accomplished in a series of 11 steps, each going from $\varphi = e\%$ to $\varphi = 1\%$, the out-percolation time is 198 Ma. This huge disparity arises because t_p is inversely proportional to k, which probably scales as φ^3 (Wark and Watson, 1998; Zhu and Hirth, 2003). In the high initial φ model, most of the aggregate melt removal happens at very high ω; the last 9% of melt removal, at slower and still steadily diminishing ω, takes 87% of the total t_p. In the never-high-φ model, the average ω is the same as in that last slow-ω 9% of melt removal in the high initial φ model.

These are merely examples, and the absolute values of the t_p durations are subject to considerable uncertainty (e.g., real ureilite mafic silicates are not all 1-mm radius spheres; μ might have been reduced by extraordinarily high C and S; melt out-percolation was possibly aided by sporadic impacts, cracking, etc.). Nonetheless, the percolation-compaction constraint clearly favors a moderate-to-high φ during ureilite anatexis, and militates against an extreme fractional style of melting. The heat source for asteroidal melting is not well known (Rubin, 2006, advocates impact-heating for ureilites). But there is abundant evidence that ^{53}Mn ($t_{1/2} = 3.7$ Ma) and even ^{26}Al (0.73 Ma) were alive when asteroidal basalts (eucrites and angrites) were forming (Lugmair and Shukolyukov, 1998; Srinivasan et al., 1999; Nyquist et al., 2001, 2003); and Kita et al. (2003) extended this to a basaltic clast in polymict ureilite DaG 319. Even if the main heat source was not, as widely assumed, ^{26}Al, it manifestly lost its efficacy on a time scale of the order of the half-life of ^{26}Al. Plausible ureilite petrogenesis models should not require many tens of Ma for a slow, fractional purge of basalt from the nascent restite. More plausible are models that assume f managed to reach a considerable fraction, at least, of the ~20% inferred aggregate basalt removed, before the rate of melt out-flow began to outpace the rate of melt generation.

7.4. Incompatible trace elements

In this section, we use incompatible trace elements to constrain f during the anatexis that produced the ureilites. This general approach has been used before (e.g., Warren and Kallemeyn, 1992), but here we incorporate better constraints on the ureilite compositions, and a more sophisticated model for the melting process. We will focus on Sm, a moderately incompatible element that conveniently is often determined in ureilites, and in melt-mineral partitioning experiments. More extremely incompatible elements are not preferable, for this purpose, because they occur at extremely low concentration in ureilites and yet are very enriched in Earth's crust, making them severely contamination-prone. We will explicitly discuss only the data for residues from acid-leaching experiments, which by design strip away the terrestrial contaminants (typically the residue is about 1/2 as Sm-rich as the untreated bulk rock), and hopefully do not also remove significant indigenous Sm. This approach conservatively downplays the possibility that incompatible elements tended to be concentrated in portions of the pre-terrestrial ureilites that were derived from "trapped" restitic melt and thus were interstitial and fine-grained, i.e., leach-prone.

Leaching experiments involving Sm have been reported (Spitz and Boynton, 1991; Goodrich and Lugmair, 1992, 1995; Kita et al., 1995) for ALHA77257, ALHA81101, ALH82106/4136, Goalpara, Kenna and PCA82506. All of these except ALH82106/4136 are olivine-pigeonite ureilites. The simple average of all the residue-Sm results, with pre-averaging for each of the six studied ureilites, is 0.053× CI chondrites (Fig. 11). The average excluding the augite-bearing ALH82106/4136 is 0.024 × CI. Note that 4/5 of the olivine-pigeonite leaching experiments have been done on uncommonly Sm-poor samples. Thus, despite great scatter in the residue data, 0.024× CI seems a conservatively low estimate for the average pre-terrestrial Sm concentration in olivine–pigeonite ureilites.

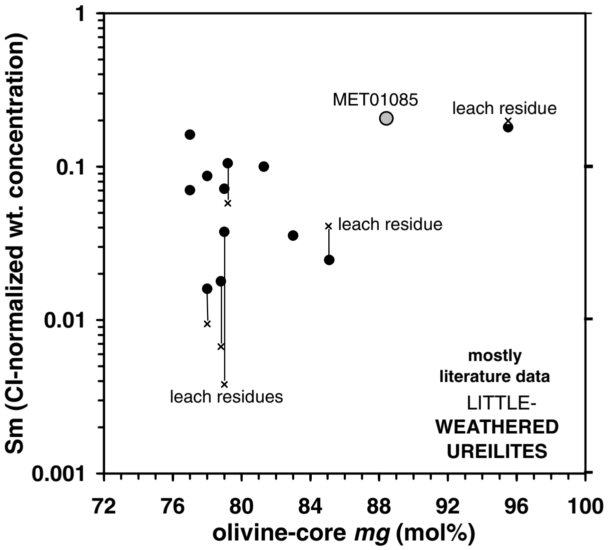

Fig. 11. Olivine-core *mg* vs. bulk-rock Sm concentration in little-weathered ureilites and leach-experiment residues. Residue data are from Spitz and Boynton (1991) for ALHA77257, ALHA81101, ALH82106/4136, Kenna and PCA82506; from Kita et al. (1995) for Goalpara; and from Goodrich and Lugmair (1992, 1995) for Kenna and PCA82506.

To construct partial melting models for these compositions, we assume the starting material was a chondrite-like peridotite with 60 wt% olivine, 27 wt% pigeonite, 12 wt% plagioclase, plus minor augite and ilmenite. Melting is assumed to be nonmodal, but (conservatively) only in terms of the proportion of plagioclase to mafic silicates; the olivine/pigeonite/augite/ilmenite proportionality is not varied. Crystal/melt D values are assumed to be 0.00084 for olivine (McKay, 1986; Nielsen et al., 1992; Kennedy et al., 1993), 0.025 for pigeonite (McKay et al., 1986), 0.018 for plagioclase (Phinney and Morrison, 1990), and 0.31 for the trace of augite (numerous sources). The final, aggregate degree of partial melting was assumed to be 20 wt%, based on mass balance for Al (see above).

Besides the classical equilibrium ("batch") and fractional (Rayleigh) partial melting models, we calculated a series of "continuous" partial melting models. These assume that melt continuously bled out of the source, as in fractional melting, but also continuously left a few percent of residual melt porosity φ in the source. Physically, continuous melting is probably more realistic, for most contexts, than either "batch" or fractional melting (as the assumed residual porosity approaches zero, continuous melting converges toward fractional melting). Equations for continuous melting have been published in, e.g., Albarède (1995). Finally, as a special model potentially appropriate to ureilites, we modified the continuous models by assuming that after all melting ceased, the residual melt porosity (φ) was abruptly reduced to 1–2 wt%. This step is meant to simulate the terminal purging of the ureilites that, as discussed in the previous section, was probably facilitated by catastrophic disruption of the parent body(ies).

Results are shown in Fig. 12. Assuming the available leach-residue data are representative, the equilibrium model predicts a too-high Sm concentration for the olivine–pigeonite ureilites. The end-member fractional fusion model grossly under-predicts Sm, by ~5 orders of magnitude. The continuous-melting model matches the conservatively estimated leach-residue average when the continuous melt porosity φ is ~5 wt%. The continuous-and-late-purge model matches the leach-residue average when $\varphi \sim 10$ wt%. The 5 wt% result should probably be viewed as a lower limit on the average melt porosity during ureilite anatexis, because using only the leach-residue results from consistently Sm-poor olivine–pigeonites may well have biased the sample average toward low Sm (and certainly did not bias it toward high Sm). The true average melt porosity during anatexis could easily have been well over 10 wt%.

As an argument in favor of fractional melting, Goodrich et al. (2004) suggested that incompatible elements might have failed to equilibrate during ureilite anatexis, because melt "extraction" (accelerated by escaping CO gas from smelting) was too rapid for chemical equilibration. To prevent equilibration, however, some special circumstance of ureilite anatexis would have to accelerate the process of melt *generation*, not just melt extraction. Extraordinarily rapid extraction would only tend to maintain the melt/crystals equilibrium established during anatexis. Indeed, rapid extraction of melt from a mantle source region is a prerequisite for eruption of (ideally) "primary" basalt. The smelting reaction, Eq. (1), is endothermic; so smelting, even in a spurt associated with catastrophic break-up of the parent asteroid, would not accelerate melt generation, only melt extraction.

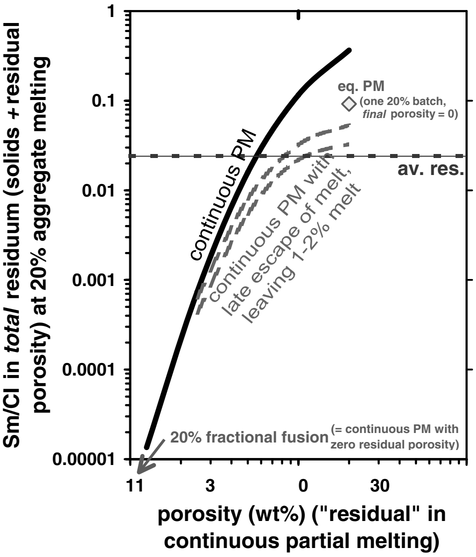

Fig. 12. Anatectic-melt porosity vs. CI-chondrite-normalized Sm concentration in total restite (solids + residual porosity) at 20% aggregate melting, calculated by various models (see text). Continuous partial melting is generally more physically realistic than either ideal equilibrium ("eq.") partial melting or fractional fusion. Also shown are ureilite-specific models that assume continuous partial melting was followed by a large purging of the melt porosity. Models match the average Sm in ureilite leach-residues ("av. res."; conservatively estimated, see text) only if the anatectic-melt porosity is assumed to have been at least 5 wt%.

In conclusion, available temporal, physical and trace-element constraints seem consistent with a moderate, of order 10 wt%, silicate-melt porosity during the ureilite anatexis. This proportion of melt would probably be enough to allow S-rich metallic melt to migrate efficiently, but not so large that efficient entrainment of solid FeNi would also occur. Finally, it should be noted that if Yoshino et al. (2004) have correctly assessed the threshold for Fe–S melt percolation, the ureilite siderophile data, by themselves, imply that the anatectic melt porosity must have been high.

7.5. *Fate of the metallic melt*

It is not entirely clear that the S-rich metallic melt we infer separated from the anatectic ureilites ended up wholly, or even predominantly, within the asteroidal core. Keil and Wilson (1993) suggested that the early S-rich metallic melts on some asteroids were so uniformly mingled with gas bubbles that they were (in effect) positively buoyant, and therefore instead of contributing to the asteroidal core they mainly migrated upward, and were ultimately launched permanently off the asteroid by gas-expansion explosive volcanism (cf. the Wilson and Keil, 1991, model for asteroidal basalt-loss). Goodrich et al. (2004) suggested (briefly) that this process might have removed the Fe-metal that should have formed, and yet is not found among even polymict ureilites, as a result of the smelted-cores scenario. In the Keil and Wilson (1993) model, initial melt migration is assumed to be through veins that open when Fe–FeS melting creates a region of excess pressure in the asteroidal mantle. A key premise of this model is that the gas remains dispersed throughout the ascending melt during the entire journey from source region to surface.

Keil and Wilson (1993) admitted that in larger asteroids the gas and metallic melt would be prone to separate before they could ascend completely to the surface. They estimated a radius of 80 km as the size at which "a rapid change in average buoyancy" occurs. However, this size estimate was not based on physical modeling, but rather on a huge extrapolation from trace-element trends and metallographic cooling rates for iron meteorites (Haack et al., 1990). Unless the ureilites are (implausibly) a strongly biased sample of mainly deepest mantle materials, the minimum pressures that can be inferred from their core *mg* ratios (greater than about 20–25 bars for the most magnesian ureilites, or about 70 bars for typical ureilites: Warren and Kallemeyn, 1992; Walker and Grove, 1993) suggest that the parent asteroid(s) were at least 100 km in radius. The ureilite asteroid(s) was probably large enough for its metallic melts to generally descend into a nascent core.

7.6. Planetary implications

The ureilite siderophile, chalcophile, and S data suggest that core formation, at least in asteroids, probably occurs in two discrete stages. A large proportion of S-rich metallic melt apparently managed to drain out of the anatectic mantle(s) without entraining more than a small fraction of what little Fe-metal was present. The notion (Larimer, 1995) that the entire portion of an asteroid "inside the 1000 °C isotherm…will be swept clean of its metal as well as its sulfide" is clearly contradicted by the ureilites. The extent of silicate-anatectic porosity required for a "clean sweep" of Fe-metal must be greater than the φ inferred for ureilites in the previous two sections, i.e., upwards of 5%. The required temperature must be greater than the range of 1213–1301 °C at which the ureilites equilibrated (Singletary and Grove, 2003).

Of course, the ureilites are just one variety, albeit a numerous and in many ways diverse variety, of achondrite. The φ and temperature thresholds for core formation must vary, depending upon compositional traits (most obviously, S and Fe-metal abundance) as well as size of the body. But assuming multi-stage core formation is the rule rather than an exception, then once a mantle has acquired a depleted S/metal ratio, whether by drain-out of S-rich metallic melt or perhaps some other process, its Fe-metal component will remain mostly solid, and thus difficult to separate from silicates, even at high temperatures that would by themselves suggest a high-φ style of anatexis. For example, assuming a negligibly low pressure and that the S/Fe-metal weight ratio has been depleted to 0.04, there would be more solid Fe-metal than metallic melt up to ~1380 °C; depletion of S/Fe-metal to 0.02 would imply ~1480 °C (Fei et al., 1997). In general, the temperature threshold for complete segregation of all Fe-metal into an asteroidal core is probably much higher than typically assumed in igneous-thermal evolution models (e.g., Ghosh and McSween, 1998). The inference that several distinct S-poor cores were producers of magmatic iron meteorites (e.g., Keil and Wilson, 1993) can be viewed as indirect evidence for remarkably extensive melting (verging on "magma ocean" extent) as a common development among moderately large asteroids.

Keil and Wilson (1993) invoked S-loss by explosive volcanism to account for surprisingly low S contents inferred for the asteroidal cores parental to some specific types of magmatic iron meteorites. Our ureilite observations suggest that S-depleted cores might instead, or also, have developed as a result of impact-disruption of growing planetesimals. Assume a disruptive event occurred when a planetesimal had reached a state of incomplete core formation, with most of the S sequestered into a metallic melt core and yet most of the solid Fe-metal (in this respect the metal-poor ureilites are admittedly not close analogs) still dispersed within the anatectic mantle. If after the disruptive impact the materials reaccreted into multiple second-generation planetesimals, nearly all of the S might have wound up in one planetesimal (the core of S-rich metallic melt remaining nearly intact) and most of the Fe-metal might have wound up in a small number of other second-generation planetesimals. Continued heating of one of these second-generation planetesimals, or an accretionary combination of several, could eventually have led to the formation of an S-poor metallic core.

8. Conclusions

1. New data for 25 ureilites to some extent mitigate the problem of extreme Al (basalt) depletion among the population of ureilites. However, the average ureilite Al concentration is still remarkably low (0.30 wt%), and probably reflects systematic depletion of the basalt component of the parent asteroid(s) by CO-fueled, Wilson and Keil (1991) style explosive volcanism.
2. Siderophile data militate against formation of any of the ureilites as conventional cumulates. None have the expected low siderophile abundances, and LEW88774, in particular, retains near-chondritic abundances of the extremely siderophile elements Ir and Os. Possibly a few ureilites are "paracumulates," i.e., reflect limited crystal-melt segregation on a highly localized scale, where regions of exceptionally high melt fraction happened to develop, stochastically and temporarily, within the anatectic mantle.

3. Mass/volume balance for CO gas represents the most severe problem with the notion that pressure-buffered smelting determined the *mg* of the ureilites' mafic-silicate cores. Even supposing that the copious volume of CO gas generated by smelting leaked out of the mantle, the smelted-cores model also predicts production of several wt% Fe-metal. None of the ureilites, least of all the ureilite with the most "reduced" (highest) olivine-core *mg* (ALH84136), have the predicted Fe-metal abundance. In principle, the Fe-metal generated by smelting could have been subsequently lost, but siderophile data show that ureilites like ALH84136 never underwent efficient depletion of Fe-metal.
4. The ureilites display good correlations among siderophile ratios such as Au/Ir, Ni/Ir, Co/Ir, As/Ir, Se/Ir, and Sb/Ir. The pattern of ureilite siderophile depletions shows significant resemblance to siderophile fractionations, presumably nebular in origin, among the carbonaceous chondrites. But zinc, and to a lesser degree Ge, are anomalously high in ureilites compared to other elements of comparable volatility.
5. The well-defined correlation between Au and Ni extrapolates significantly to the low-Ni/Au side of the compositional range of carbonaceous chondrites. This mismatch, along with mild but nonetheless significant depletions of refractory siderophile elements such as Ir and Os, and moderate depletions of strongly siderophile, weakly chalcophile elements such as Ni and Au, all suggest that the siderophile fractionations among ureilites are at least largely the result of a secondary, non-nebular process, i.e., removal of S-rich metallic melt, possibly with minor entrainment of Fe-metal.
6. More $D_{\mathrm{ml/sm}}$ data are needed for chalcophile, weakly siderophile elements such Cd, In, and especially Zn.
7. Apart from the siderophile depletions themselves, two lines of evidence suggest that melt porosity φ during ureilite anatexis must have been at least moderate. Unless φ was at least several wt%, a prohibitively long time is required for out-percolation of the ~20 wt% (minimum) of basaltic melt that Al mass balance suggests separated from the ureilite-asteroidal mantle(s). Also, incompatible element depletions are moderate enough to imply that the average (silicate) φ was at least several wt%.
8. The prevalent ureilite siderophile pattern (very mild depletions of extremely siderophile elements, much deeper depletions of chalcophile, weakly siderophile elements) suggests that core formation, at least in asteroid-sized bodies, probably occurs in two discrete stages. In general, separation of a considerable proportion (several wt%) of S-rich metallic melt probably occurs long before, and at far lower T than, separation of the remaining S-poor Fe-metal. Apart from the Fe-metal itself, only extremely siderophile elements (not, e.g., Ni nor Au) wait until the second stage to sequester mainly into the core.

Acknowledgments

We thank N.L. Chabot and E. Cottrell for helpful, constructive reviews. We also thank the Meteorite Working Group, the Japanese NIPR, M. Farmer, N. Gessler, D. Gregory, and E. Thompson for generous loans and donations of samples. This work was supported by NASA Grant NAG5-12819.

Associate editor: Richard J. Walker

References

Albarède, F., 1995. *Introduction to Geochemical Modeling*. Cambridge University Press, Cambridge, UK.

Berkley, J.L., Jones, J.H., 1982. Primary igneous carbon in ureilites: petrological implications. *Proc. Lunar Planet. Sci. Conf.* **13**, A353–A364.

Berkley, J.L., Taylor, G.J., Keil, K., Harlow, G.E., Prinz, M., 1980. The nature and origin of ureilites. *Geochim. Cosmochim. Acta* **44**, 1579–1597.

Binz, C.M., Ikramuddin, M., Lipschutz, M.E., 1975. Contents of eleven trace elements in ureilite achondrites. *Geochim. Cosmochim. Acta* **39**, 1576–1579.

Bland, P.A., 1993. FRO90168. *Euromet Bull.* **2** (1), 5.

Borisov, A., Palme, H., 1995. The solubility of iridium in silicate melts: new data from experiments with Ir10Pt90 alloys. *Geochim. Cosmochim. Acta* **59**, 481–485.

Boynton, W.V., Hill, D.H., 1993. Trace-element abundances in several new ureilites (abstract). *Lunar Planet. Sci.* **24**, 167–168.

Boynton, W.V., Starzyk, P.M., Schmitt, R.A., 1976. Chemical evidence for the genesis of the ureilites, the achondrite Chassigny and the nakhlites. *Geochim. Cosmochim. Acta* **40**, 1439–1447.

Chabot, N.L., Jones, J.H., 2003. The parameterization of solid metal–liquid metal partitioning of siderophile elements. *Meteorit. Planet. Sci.* **38**, 1425–1436.

Chabot, N.L., Campbell, A.J., Jones, J.H., Humayun, M., Agee, C.B., 2006. An experimental test of Henry's Law in solid metal–liquid metal systems with implications for iron meteorites. *Meteorit. Planet. Sci.* **38**, 181–196.

Chabot, N.L., Campbell, A.J., Jones, J.H., Humayun, M., Lauer, H.V., 2006. The influence of carbon on partitioning behavior during planetary evolution. *Geochim. Cosmochim. Acta*, **70**, 1322–1335.

Chikami, J., Mikouchi, T., Takeda, H., Miyamoto, M., 1997. Mineralogy and cooling history of the calcium–aluminum–chromium enriched ureilte, LEW88774. *Meteorit. Planet. Sci.* **32**, 343–348.

Clayton, R.N., Mayeda, T.K., 1988. Formation of ureilites by nebular processes. *Geochim. Cosmochim. Acta* **52**, 1313–1318.

Fei, Y., Bertka, C.M., Finger, L.W., 1997. High-pressure iron sulfur compound, Fe_3S_2, and melting relations in the Fe–FeS system. *Science* **275**, 1621–1623.

Sexton, I.A., Wright, A.S., Pillinger, I.P., Franchi, C.T., 1998. Oxygen isotopic homogeneity in the ureilite population (abstract 1685)*Lunar and Planetary Science*, vol. 29. Lunar and Planetary Institute (CD-ROM).

Ghosh, A., McSween Jr., H.Y, 1998. A thermal model for the differentiation of asteroid 4 Vesta, based on radiogenic heating. *ICARUS* **134**, 187–206.

Gillum, D.E., Janghorbani, M., Miller, M.D., Chyi, L.L., Ehmann, W.D., 1972. Elemental abundances in the Haverö meteorite. *Meteoritics* **7**, 573–578.

Goodrich, C.A., 1992. Ureilites: a critical review. *Meteoritics* **27**, 327–352.

Goodrich, C.A., 1999. Are ureilites residues from partial melting of chondritic material? The answer from MAGPOX. *Meteorit. Planet. Sci.* **34**, 109–119.

Goodrich, C.A., 2001. Mamgatic inclusions in Frontier Mountains 90054 and Elephant Moraine 96328: complex petrogenesis of the olivine-(augite)-orthopyroxene ureilites (abstract 1300), Lunar and Planetary Institute (CD-ROM).*Lunar and Planetary Science*, vol. 32.

Goodrich, C.A., Berkley, J.L., 1986. Primary magmatic carbon in ureilites: evidence from cohenite-bearing metallic spherules. *Geochim. Cosmochim. Acta* **50**, 681–691.

Goodrich, C.A., Harlow, G.E., 2001. Knorringite–uvavorite garnet and Cr-Eskola pyroxene in ureilite LEW88774 (abstract). *Meteorit. Planet. Sci.* **36**, A68.

Goodrich, C.A., Keller, L.P., 2000. Transmission electron microscope investigation of a silicate mineral/melt reaction texture in ureilite Lewis Cliff 88774 (abstract). *Meteorit. Planet. Sci.* **35**, A60–A61.

Goodrich, C.A., Lugmair, G.W., 1992. Sm–Nd and Rb–Sr isotopic systematics of ureilites. *Geochim. Cosmochim. Acta* **55**, 829–848.

Goodrich, C.A., Lugmair, G.W., 1995. Stalking the LREE-enriched component in ureilites. *Geochim. Cosmochim. Acta* **59**, 2609–2620.

Goodrich, C.A., Fioretti, A.M., Tribaudino, M., Molin, G., 2001. Primary trapped melt inclusions in olivine in the olivine–augite–orthopyroxene ureilite Hughes 009. *Geochim. Cosmochim. Acta* **65**, 621–652.

Goodrich, C.A., Jones, J.H., Berkley, J.L., 1987. Origin and evolution of the ureilite parent magmas: multi-stage igneous activity on a large parent body. *Geochim. Cosmochim. Acta* **51**, 2255–2273.

Goodrich, C.A., Scott, E.R.D., Fioretti, A.M., 2004. Ureilitic breccias: clues to the petrologic structure and impact disruption of the ureilite parent asteroid. *Chem. Erde* **64**, 283–327.

Grady, M.M., Pillinger, C.T., 1993. Euromet ureilite consortium: a preliminary report on carbon and nitrogen geochemistry (abstract). *Lunar Planet. Sci.* **24**, 551–552.

Grady, M.M., Wright, I.P., Swart, P.K., Pillinger, C.T., 1985. Carbon and nitrogen isotopic composition of ureilites: implications for their genesis. *Geochim. Cosmochim. Acta* **49**, 903–915.

Grossman, J.N., Baedecker, P.N., 1986. Computer graphics for quality control in the INAA of geological samples. In: *Proceedings of the Seventh International Conference on Modern Trends in Activation Analysis*, pp. 571–578.

Haack, H., Rasmussen, K.L., Warren, P.H., 1990. Effects of regolith/megaregolith development on the cooling histories of differentiated asteroids. *J. Geophys. Res.* **95**, 5111–5124.

Herpfer, M.A., Larimer, J.W., 1993. Core formation: an experimental study of metallic melt-silicate segregation (abstract). *Meteoritics* **26**, 362.

Higuchi, H., Morgan, J.W., Ganapathy, R., Anders, E., 1976. Chemical fractionations in meteorites—X. Ureilites. *Geochim. Cosmochim. Acta* **40**, 1563–1571.

Hintenberger, H., Jochum, K.P., Braun, O., Christ, P., Martin, W., 1978. The Antarctic meteorite Yamato 74123—a new ureilite. *Earth Planet. Sci. Lett.* **40**, 187–193.

Hudon, P., Mittlefehldt, D.W., 2004. Ureilite geochemistry and smelting (abstract). *Meteorit. Planet. Sci.* **39**, A48.

Hunter, R.H., 1996. Texture development in cumulate rocks. In: Cawthorn, R.G. (Ed.), *Layered Intrusions*. Elsevier, Amsterdam, pp. 77–101.

Ikeda, Y., Prinz, M., 2001. Magmatic inclusions and felsic clasts in the Dar al Gani 319 polymict ureilite. *Meteorit. Planet. Sci.* **36**, 481–499.

Janssens, M.-J., Hetrogen, J., Wolf, R., Ebihara, M., Anders, E., 1987. Ureilites: trace element clues to their origin. *Geochim. Cosmochim. Acta* **51**, 2275–2283.

Jaques, A.L., Fitzgerald, M.J., 1982. The Nilpena ureilite, an unusual polymict breccia: implications for origin. *Geochim. Cosmochim. Acta* **46**, 893–900.

Jarosewich, E., 1990. Chemical analyses of meteorites: a compilation of stony and iron meteorite analyses. *Meteoritics* **25**, 323–337.

Jerome, D.Y., 1970. *Composition and origin of some achondritic meteorites*. Ph.D. Thesis, University of Oregon, Eugene.

Jones, J.H., Beattie, P., Jurewicz, A.J.G., Lauer Jr., H.V., Le, L., Lindstrom, D.J., Norman, M.D., Wagstaff, J.H., Walker, D., Walker, R.J., 1997. Partitioning of Re, Os, and Ir between metal and silicate liquid (abstract). *Lunar Planet. Sci.* **28**, 677–678.

Jurewicz, A.J.G., Mittlefehldt, D.W., Jones, J.H., 1995. Experimental partial melting of the St. Severin (LL) and Lost City (H) chondrites. *Geochim. Cosmochim. Acta* **59**, 391–408.

Kaiura, G.H., Toguri, J.M., 1979. Densities of the molten FeS, FeS–Cu_2S and Fe–S–O systems-utilizing a bottom-balance Archimediam technique. *Can. Metall. Quart.* **18**, 155–164.

Kallemeyn, G.W., 1993. Neutron activation analysis. In: Hyman, M., Rowe, M.W. (Eds.), *Advances in Analytical Chemistry*. JAI Press, Greenwich, CT, pp. 193–209.

Kallemeyn, G.W., Rubin, A.E., Wasson, J.T., 1994. The compositional classification of chondrites: VI. The CR carbonaceous chondrite group. *Geochim. Cosmochim. Acta* **58**, 2873–2888.

Keil, K., Wilson, L., 1993. Explosive volcanism and the compositions of cores of differentiated asteroids. *Earth Planet. Sci. Lett.* **117**, 111–124.

Kennedy, A.K., Lofgren, G.E., Wasserburg, G.J., 1993. An experimental study of trace element partitioning between olivine, orthopyroxene, and melt in chondrules. *Earth Planet. Sci. Lett.* **115**, 177–195.

Kita, N.T., Ikeda, Y., Shimoda, H., Morishita, Y., Togashi, S., 2003. Timing of basaltic volcanism in ureilite parent body inferred from the ^{26}Al ages of plagioclase-bearing clasts in DaG-319 polymict ureilite (abstract 1557)*Lunar and Planetary Science*, vol. 34. Lunar and Planetary Institute (CD-ROM).

Kita, N.T., Ikeda, Y., Togashi, S., Liu, Y., Morishita, Y., Weisberg, M.K., 2004. Origin of ureilites inferred from a SIMS oxygen isotopic and trace element study of clasts in the Dar al Gani 319 polymict ureilite. *Geochim. Cosmochim. Acta* **68**, 4213–4235.

Kita, N.T., Misawa, K., Tatsumoto, M., 1995. U–Th–Pb and Sm–Nd isotopic systematics of the Goalpara ureilite: resolution of terrestrial contamination. *Geochim. Cosmochim. Acta* **59**, 381–390.

Larimer, J.W., 1995. Core formation in asteroid-sized bodies. *Meteoritics* **30**, 533.

Lebedev, E.B., Kadik, A.A., Kuskov, O.L., Dorfman, A.M., Lukanin, O.A., 1999. The motion of sulfide phases in a partially molten silicate material: application to the problem of the formation of planetary cores. *Astronom. Vest.* **33**, 346–356.

Lugmair, G.W., Shukolyukov, A., 1998. Early solar system timescales according to ^{53}Mn–^{53}Cr systematics. *Geochim. Cosmochim. Acta* **62**, 2863–2886.

McCall, G.J.H., Cleverly, W.H., 1968. New stony meteorite finds including two ureilites from the Nullarbor Plain, Western Australia. *Mineral. Mag.* **36**, 691–716.

McCoy, T., Benedix, G., Welzenbach, L., 2002. MET01085 thin section description. *Antarct. Meteori. Newsl.* **25** (2) (no pagination).

McKay, G.A., 1986. Crystal/liquid partitioning of REE in basaltic systems: extreme fractionation of REE in olivine. *Geochim. Cosmochim. Acta* **50**, 69–79.

McKay, G.A., Wagstaff, J., Yang, S.-R., 1986. Clinopyroxene REE distribution coefficients for shergottites: the REE content of the Shergotty melt. *Geochim. Cosmochim. Acta* **50**, 927–937.

McKenzie, D., 1989. Some remarks on the movement of small melt fractions in the mantle. *Earth Planet. Sci. Lett.* **95**, 53–72.

Mittlefehldt, D.W., Hudon, P., Galdino Jr, C., 2005. Petrology, geochemistry and genesis of ureilites (abstract 1040)*Lunar and Planetary Science*, vol. 36. Lunar and Planetary Institute (CD-ROM).

Mittlefehldt, D.W., McCoy, T.J., Goodrich, C.A., Kracher, A., 1998. Non-chondritic meteorites from asteroidal bodies. In: Papike, J.J. (Ed.), *Planetary Materials, Reviews in Mineralogy*, vol. 36. Mineralogical Society of America, pp. 4.1–4.195.

Nagamori, M., 1969. Density of molten Ag–S, Cu–S, Fe–S, and Ni–S systems. *Trans. Metallurg. Soc. AIME* **245**, 1897–1902.

Nielsen, R.L., Gallahan, W.E., Newberger, F., 1992. Experimentally determined mineral-melt partition coefficients for Sc, Y and REE for olivine, orthopyroxene, pigeonite, magnetite and ilmenite. *Contrib. Mineral. Petrol.* **110**, 488–499.

Nyquist, L.E., Shih, C-Y., Wiesmann, H., Mikouchi, T., 2003. Fossil ^{26}Al and ^{53}Mn in D'Orbigny and Sahara 99555 and the timescale for angrite magmatism (abstract 1388)*Lunar and Planetary Science*, vol. 34. Lunar and Planetary Institute (CD-ROM).

Nyquist, L.E., Reese, Y., Wiesmann, H., Shih, C.-Y., Takeda, H., 2001. Live ^{53}Mn and ^{26}Al in an unique cumulate eucrite with very calcic feldspar (An-98) (abstract). *Meteor. Planet. Sci.* **36**, A151–A152.

Phinney, W.C., Morrison, D.A., 1990. Partition coefficients for calcic plagiolcase: implications for Archean anorthosites. *Geochim. Cosmochim. Acta* **54**, 2025–2043.

Rankenburg, K., Brandon, A.D., Humayun, M., 2005. Highly siderophile elements and osmium isotope systematics in ureilites: are the carbonaceous veins primary components? (Abstract 1224)*Lunar and Planetary Science*, vol. 36. Lunar and Planetary Institute (CD-ROM).

Righter, K., 2003. Metal-silicate partitioning of siderophile elements and core formation in the early Earth. *Ann. Rev. Earth Planet. Sci.* **31**, 135–174.

Rubin, A.E., 2006. Shock, post-shock annealing and post-annealing shock in ureilites. *Meteorit. Planet. Sci.* **41**, 125–134.

Rushmer, T., Humayun, M., Campbell, A.J., 2004. Siderophile element abundances in Fe–S–Ni–O melts segregated from partially molten ordinary chondrite under dynamic conditions (abstract 1850)*Lunar and Planetary Science*, vol. 35. Lunar and Planetary Institute (CD-ROM).

Rushmer, T., Minarik, W.G., Taylor, G.J., 2000. Physical processes of core formation. In: Canup, R.M., Righter, K. (Eds.), *Origin of the Earth and Moon*. University of Arizona Press, Tucson, pp. 227–243.

Schmitt, R.A., Goles, G.G., Smith, R.H., Osborn, T.W., 1972. Elemental abundances in stone meteorites. *Meteoritics* **7**, 131–214.

Scott, E.R.D., Taylor, J.G., Keil, K., 1993. Origin of ureilite meteorites and implications for planetary accretion. *Geophys. Res. Lett.* **20**, 415–418.

Shaw, H.R., 1972. Viscosities of magmatic silicate liquids: an empirical method of prediction. *Am. J. Sci.* **272**, 870–893.

Shirley, D.N., 1986. Differentiation and compaction in the Palisades Sill, New Jersey. *J. Petrol.* **28**, 835–865.

Sikirdji, M., Warren, P.H., 2001. Northwest Africa 766: a new ferroan ureilite with Cr-spinel, Cr-rich garnet (?) and associated Si,Al-rich glasses (abstract). *Meteorit. Planet. Sci.* **36**, A189.

Singletary, S.J., Grove, T.L., 2003. Early petrogenetic processes on the ureilite parent body. *Meteorit. Planet. Sci.* **38**, 95–108.

Smith, C.L., Franchi, I.A., Wright, I.P., Grady, M.M., Pillinger, C.T., 2001. New data on carbon isotopic compositions of ureilites (abstract 1878)*Lunar and Planetary Science*, vol. 32. Lunar and Planetary Institute (CD-ROM).

Smith, C.L., Wright, I.P., Franchi, I.A., Grady, M.M., 2000. A statistical analysis of mineralogical data from Frontier Mountain ureilites (abstract). *Meteorit. Planet. Sci.* **35**, A150.

Spitz, A.H., 1992. ICP-MS trace element analysis of ureilites: evidence for mixing of distinct components (abstract). *Lunar Planet. Sci.* **23**, 1339–1340.

Spitz, A.H., Boynton, W.V., 1991. Trace element analysis of ureilites: new constraints on their petrogenesis. *Geochim. Cosmochim. Acta* **55**, 3417–3430.

Srinivasan, G., Goswami, J.N., Bhandari, N., 1999. ^{26}Al in eucrite Piplia Kalan: plausible heat source and formation chronology. *Science* **284**, 1348–1350.

Takeda, H., 1987. Mineralogy of Antarctic ureilites and a working hypothesis for their origin and evolution. *Earth Planet. Sci. Lett.* **81**, 358–370.

Takeda, H., Mori, H., Ogata, H., 1989. Mineralogy of augite-bearing ureilites and the origin of their chemical trends. *Meteoritics* **24**, 73–81.

Thrush, P.W. (Ed.), 1968. *A Dictionary of Mining, Mineral, and Related Terms*. U.S. Department of the Interior, Bureau of Mines, U.S. Government Printing Office, p. 1269.

Usselman, T.M., 1975. Experimental approach to the state of the core: Part II. Composition and thermal regime. *Am. J. Sci.* **275**, 291–303.

Wager, L.R., Brown, G.M., 1967. *Layered Igneous Rocks*. Freeman, New York, p. 588.

Walker, D., Agee, C.B., 1988. Ureilite compaction. *Meteoritics* **23**, 81–91.

Walker, D., Grove, T., 1993. Ureilite smelting. *Meteoritics* **28**, 629–636.

Walter, M.J., Newsom, H.E., Ertel, W., Holzheid, A., 2000. Siderophile elements in the Earth and Moon: metal/silicate partitioning and implications for core formation. In: Canup, R.M., Righter, K. (Eds.), *Origin of the Earth and Moon*. University of Arizona Press, pp. 265–289 (N).

Wang, M.-S., Lipschutz, M.E., 1995. Volatile trace elements in Antarctic ureilites. *Meteoritics* **30**, 319–324.

Wark, D.A., Watson, E.B., 1998. Grain-scale permeabilities of texturally equilibrated, monomineralic rocks. *Earth Planet. Sci. Lett.* **164**, 591–605.

Warren, P.H., 1996. Ureilite origin by "smelting": a conceptual pitfall (abstract). *Meteorit. Planet. Sci.* **31**, A146.

Warren, P.H., 2004. Complex, contrasting behavior of chromium during late-stage processes in ureilites (abstract 2151)*Lunar and Planetary Science*, vol. 35. Lunar and Planetary Institute (CD-ROM).

Warren, P.H., Huber, H., 2006. Ureilite "smelting" and the catastrophic disruption hypothesis. *Meteorit. Planet. Sci.* **40**, in press.

Warren, P.H., Huber, H., Ulff-Møller, F., 2006. Alkali-feldspathic material entrained in Fe,S-rich veins in a monomict ureilite. *Meteorit. Planet. Sci.*, **40**, in press.

Warren, P.H., Kallemeyn, G.W., 1989. Geochemistry of polymict ureilite EET83309, and a partially-disruptive impact model for ureilite origin. *Meteoritics* **24**, 233–246.

Warren, P.H., Kallemeyn, G.W., 1992. Explosive volcanism and the graphite-oxygen fugacity buffer on the parent asteroid(s) of the ureilite meteorites. *ICARUS* **100**, 110–126.

Warren, P.H., Kallemeyn, G.W., Kyte, F.T., 1999. Origin of planetary cores: evidence from highly siderophile elements in martian meteorites. *Geochim. Cosmochim. Acta* **63**, 2105–2122.

Wasson, J.T., 1985. *Meteorites: Their Record of Early Solar System History*. Freeman, New York, p. 267.

Wasson, J.T., Kallemeyn, G.W., 1988. Compositions of chondrites. *Philos. Trans. R. Soc. Lond. A* **325**, 535–544.

Wasson, J.T., Chou, C.L., Bild, R.W., Baedecker, P.A., 1976. Classification of and elemental fractionation among ureilites. *Geochim. Cosmochim. Acta* **40**, 1449–1458.

Wiik, H.B., 1972. The chemical composition of the Haverö meteorite and the genesis of the ureilites. *Meteoritics* **7**, 553–557.

Wilson, L., Keil, K., 1991. Consequences of explosive eruptions on small Solar System bodies: the case of the missing basalts on the aubrite parent body. *Earth Planet. Sci. Lett.* **104**, 505–512.

Wlotzka, F., 1972. Haverö ureilite: evidence for recrystallization and partial reduction. *Meteoritics* **7**, 591–600.

Wlotzka, F., 1993. A weathering scale for the ordinary chondrites (abstract). *Meteoritics* **28**, 460.

Xiao, X., Lipschutz, M.E., 1993. Labile trace elements in carbonaceous chondrites: a survey. *J. Geophys. Res. Planets* **97**, 10199–10211.

Yanai, K., Kojima, H., 1995. *Catalog of the Antarctic Meteorites*. National Institute of Polar Research, p. 230.

Yoshino, T., Walter, M.J., Katsura, T., 2004. Connectivity of molten Fe alloy in peridotite based on in situ electrical conductivity measurements: implications for core formation in terrestrial planets. *Earth Planet. Sci. Lett.* **222**, 625–643.

Zhu, W., Hirth, G., 2003. A network model for permeability in partially molten rocks. *Earth Planet. Sci. Lett.* **212**, 407–416.